PB-231 174

MOLECULAR MODULATION SPECTROMETRY FOR OBSERVATION OF FREE RADICALS

Harold S. Johnston

California University

Prepared for:

Environmental Protection Agency

March 1974

DISTRIBUTED BY:

NTIS

National Technical Information Service
U. S. DEPARTMENT OF COMMERCE
5285 Port Royal Road, Springfield Va. 22151

TECHNICAL REPORT DATA
(Please read Instructions on the reverse before completing)

1. REPORT NO.	2.	3. PB 231 174
EPA-650/4-74-004		

4. TITLE AND SUBTITLE	5. REPORT DATE
Molecular Modulation Spectrometry for Observation of Free Radicals	March 1974
	6. PERFORMING ORGANIZATION CODE
7. AUTHOR(S)	8. PERFORMING ORGANIZATION REPORT NO.
Harold S. Johnston	
9. PERFORMING ORGANIZATION NAME AND ADDRESS	10. PROGRAM ELEMENT NO.
Department of Chemistry University of California Berkeley, California 94720	A11008
	11. CONTRACT/GRANT NO.
	R-801120
12. SPONSORING AGENCY NAME AND ADDRESS	13. TYPE OF REPORT AND PERIOD COVERED
U. S. Environmental Protection Agency National Environmental Research Center Research Triangle Park, North Carolina 27711	Final Report
	14. SPONSORING AGENCY CODE

15. SUPPLEMENTARY NOTES

16. ABSTRACT

This report contains a description of the methodology that has been developed for measuring free radicals intermediates. The molecular modulation method developed was designed to detect and follow free radicals in photochemical reactions that are known to occur at light intensities equal to that of sunlight. The goal of the project was to detect CH_3OO and $CH_3(CO)OO$ radicals and study their kinetics. This goal was not attained. However, reaction intermediates that were studied were ClOO, ClO, HOO, and N_2O_5. The method developed can measure radicals at concentrations as low as 10^{11} particles/cc.

Reproduced by
NATIONAL TECHNICAL
INFORMATION SERVICE
U S Department of Commerce
Springfield VA 22151

17. KEY WORDS AND DOCUMENT ANALYSIS

a. DESCRIPTORS	b. IDENTIFIERS/OPEN ENDED TERMS	c. COSATI Field/Group
Free Radicals Photochemistry Atmospheric Chemistry Spectrometry		

18. DISTRIBUTION STATEMENT	19. SECURITY CLASS (This report)	21. NO. OF PAGES
Unlimited	Unclassified	104
	20. SECURITY CLASS (This page)	22. PRICE
	Unclassified	$8.25/1.45

EPA Form 2220-1 (9-73)

EPA-650/4-74-004

MOLECULAR MODULATION SPECTROMETRY FOR OBSERVATION OF FREE RADICALS

by

Harold S. Johnston

Department of Chemistry
University of California
Berkeley, California 94720

EPA Grant No. R-801120
ROAP No. 26 AAD
TASK No. 12
Program Element No. A11008

EPA Project Officer: Dr. Joseph J. Bufalini

Chemistry and Physics Laboratory
National Environmental Research Center
Research Triangle Park, North Carolina 27711

Prepared for

OFFICE OF RESEARCH AND DEVELOPMENT
U.S. ENVIRONMENTAL PROTECTION AGENCY
WASHINGTON, D.C. 20460

March 1974

1a

This report has been reviewed by the Environmental Protection Agency and approved for publication. Approval does not signify that the contents necessarily reflect the views and policies of the Agency, nor does mention of trade names or commercial products constitute endorsement or recommendation for use.

ABSTRACT

Free radical intermediates determine the mechanism of most chemical and photochemical reactions. Although some indication of these intermediates can be inferred from kinetic studies, direct observation of the free radicals is required for unambiguous understanding of the mechanism. This project has developed phase-shift methods that give both kinetic and spectroscopic data for reaction intermediates in photochemical processes. The methods have been designed to observe free radicals at about 10^{11} particles/cc, and at these very low concentrations radicals have lifetimes of about one to ten seconds. New digital phase-sensitive devices have been built to measure phase shifts at these very low frequencies. The spectrometric regions are infrared (IR), ultraviolet-visible (UV), mass (MS). The reactive intermediates observed and the various regions of spectra studied by these methods are: ClOO (IR, UV, MS), ClO (UV, MS), HOO (UV, IR), and N_2O_5 in NO_2 photolysis (IR).

This report was submitted in fulfillment of ROAP No. 26AAD, TASK 12, and Grant Number 801120 by the University of California under the partial sponsorship of the Environmental Protection Agency. Work was completed as of October 31, 1973.

CONTENTS

		Page
Abstract		iii
List of Figures		vi
List of Tables		ix
Acknowledgments		x
Sections		
I	Conclusions	1
II	Recommendations	2
III	Introduction	3
IV	Apparatus	4
V	Nature of Results	11
VI	Chlorine Oxide Radicals	33
VII	Spectra and Kinetics of the Hydroperoxyl Free Radical	52
VIII	Photolysis of Nitrogen Dioxide	74
IX	Discussion	86
X	References	90

Preceding page blank

FIGURES

No.		Page
1	Schematic Diagram of Experimental Systems with Infrared Detection of Intermediates	5
2	Schematic Diagram of the System Using the Mass Spectrometer	8
3	Phase Relations Between Photolysis Light, Reactant, and Product of a Primary Photochemical Reaction	14
4	Photochemical Reaction with Simple, Single Intermediate	16
5	Phase Relations Between Photolysis Light, Reactants, Intermediates, and Products in Complex Photochemical Reaction	18
6	The Fundamental Modulation Frequency of a Primary First-Order Radical	23
7	The Modulation of a Secondary Radical	25
8	Modulation Amplitude Relative to the Limiting Amplitude	26
9	Concentration Modulation of a Second-Order Radical	29
10	Concentration Modulation of the Product of a Second-Order Radical	31
11	ClOO Infrared Molecular Modulation Spectrum	35
12	ClO_x Modulation Spectrum in Ultraviolet	37
13	High Resolution Molecular Modulation Spectrum	38
14	Calculated Relative Modulation Amplitude for the Two ClO_x Intermediates	39
15	Spectrum of New ClO_x Species	41

FIGURES

No.		Page
16	Resolution of Complex Spectrum into Two Components	42
17	Ultraviolet Spectrum of ClOO Radical as Obtained by Two Different Procedures	43
18	Observed Points and Calculated Curves for the Phase Shift of ClO	50
19	Observed Points and Calculated Curves for the Phase Shift of ClO	51
20	The Modulated Infrared Absorption Spectrum Obtained During the Photolysis of Ozone in the Presence of Hydrogen Peroxide	55
21	Six Repetitive Scans of the Modulated Absorption Spectrum Obtained During the Photolysis of Ozone in the Presence of Hydrogen Peroxide	56
22	Eleven Repetitive Scans of the Modulated Absorption Spectrum Obtained During the Photolysis of Ozone in the Presence of Hydrogen Peroxide	57
23	The Average of Sixteen Scans of the Modulated Absorption Spectrum Obtained During the Photolysis of Ozone in the Presence of Hydrogen Peroxide	58
24	Phase Shift of the Infrared Absorption Peaks	60
25	The Modulated Ultraviolet Absorption Spectrum Obtained During the Photolysis of Hydrogen Peroxide	62
26	The Dependence of the Phase Shift of the Modulation at 2200 Å on Flashing Period.	65

FIGURES

No.		Page
27	Comparison of Radical and Reactant Amplitudes	66
28	The Modulated Absorption Phase Shifts from 2450 to 2000 Å Obtained During the Photolysis of Hydrogen Peroxide	67
29	The Modulated Absorption Amplitudes from 2450 to 2000 Å Obtained During the Photolysis of Hydrogen Peroxide	68
30	The Phase Shift of the Radical vs the Flashing Period	70
31	The Ultraviolet Spectrum of the Hydroperoxyl Radical	72
32	NO_2 Decay; Comparison of Experimental Points and Calculated Curve	77
33	N_2O_5 Decay As Observed by Infrared Absorption	78
34	Concentration Ratios Where Nitrogen Pentoxide is a Maximum	79

TABLES

No.		Page
1	Absolute Cross Section for Absorption of Ultraviolet Radiation by the Free Radical ClOO and ClO in Units of 10^{-18} cm^2	44
2	Comparison of Modulated Signal of ClO and Unmodulated Signal of Ar	46
3	Comparison of Modulated Signal of ClOO and ClO	47
4	Observed Phases As a Function of Chopping Frequency and Concentrations	49
5	Data for NO_2 Modulation At One Atmosphere Total Pressure, 24°C	82
6	Observed Rate Constant and Rate Constant Ratios	83
7	Elementary Rate Constants for Nitrogen Dioxide Photolysis, 297°K, 1 atm N_2	84

ACKNOWLEDGMENTS

The work reported here was carried out by G. E. McGraw, E. D. Morris, T. T. Paukert, L. W. Richards, J. van den Bogaerde, Ching-Hsong Wu, Leo Zafonte, and Alan Harker.

SECTION I

CONCLUSIONS

The molecular-modulation method is capable of giving quantitative data concerning free radical intermediates in photochemical reactions driven by light of moderate intensity, as in sunlight. This report gives quantitative spectroscopic data for the ClO_x free radicals, ClO and ClOO. These substances and their photochemical reactions may not be important in photochemical smog, but they have unexpectedly turned out to have possible significant effect in the photochemistry of the stratosphere. This report gives quantitative spectral and kinetic data for the hydroperoxyl free radical, HOO. This radical is undoubtedly very important in both tropospheric and stratospheric pollution.

Although this method does work and has given some quantitative data on important and elusive atmospheric species, it requires a large amount of time and effort. Radical lifetimes under atmospheric conditions may be as long as several seconds, and signal-to-noise features are extremely unfavorable at such frequencies. It is so difficult to obtain data by this method that it cannot be recommended as a general method of kinetics; it should be used only when one must study photochemical reactions under realistic atmospheric conditions.

SECTION II

RECOMMENDATIONS

If this method is to be developed further, one should go to higher intensities of photolyzing light, shorter optical paths, and faster electronics. A light intensity of about 10 to 100 times that of natural sunlight should be a fairly good simulation of realistic atmospheric conditions - it still is far less than the intensity of flash photolysis. Radical lifetimes would be 3 to 10 times shorter, and radical concentrations would be 3 to 10 times higher. If the optical path is substantially shorter, there should be less accoustical noise associated with the long lever arm of extensively folded light paths; and thus smaller modulation amplitudes should be stable.

SECTION III

INTRODUCTION

Most photochemical reactions in the gas phase occur with highly reactive free radicals as short-lived intermediates. A firm understanding of these photochemical reactions demands the direct observation of the free radicals. A considerable body of data of this kind has been built up by the method of kinetic spectroscopy and flash photolysis, which uses very high intensities of photolyzing radiation, with free radical concentrations of radicals. In this laboratory we have developed a new method that is designed to give the spectra and chemical kinetics of radicals in this range of concentration.[1] This method uses a continuous measuring probe, infrared beam, ultraviolet beam, or the collection grid of a mass spectrometer;[2-10] the photolyzing light is turned on and off at a regular controlled rate; the radicals form in the light and decay in the dark; and the continuous probe is modulated by the appearance and disappearance of radicals. This "molecular modulation" provides a differential signal that is far more sensitively observed than a direct signal. Also the step-functions of increasing products and of decreasing reactants modulate the measuring probe by about the same amount as the formation and decay of radicals. The amplitude of the modulation as a function of wave length or mass number gives the spectra of the radicals; the phase shift between photolyzing light and radical gives the lifetime, and hence the chemical kinetics, of the radical.

The photolysis of Cl_2 in the presence of O_2 was studied primarily as a check on the new apparatus, since the system has been intensively studied for more than 20 years. The hydroperoxyl radical HOO is probably the most abundant free radical in photochemical smog. The principal results of this report are quantitative infrared and ultraviolet spectra and kinetic data for the HOO free radical. This report also includes a chapter on intermediates in the photolyses of nitrogen dioxide.

SECTION IV

APPARATUS

A. INFRARED SPECTROMETER

The instrument used in this work is a long path molecular modulation infrared spectrometer. A block diagram of the apparatus is shown in Figure 1. The reaction cell is a cylindrical quartz tube 91 cm long and 28.7 cm in diameter, with a volume of 67.0 liters. The cell is equipped with gold coated multiple reflection mirrors which give it a spectroscopic path length adjustable from 4 to 40 meters. The source of the IR radiation is a Nernst glower which is chopped at 400 cps by an American Time Products tuning fork. The monochromator is a McPherson model 2051, one meter grating monochromator equipped with a 150 line per mm grating and order sorting filters. The IR detector is a liquid helium cooled, copper doped germanium photo conductor produced by the Santa Barbara Research Center.

The photolytic light for these experiments was supplied by four, 32 inch G.E. 30 watt, F30T8/BL black lamps. The photolytic photon flux in the cell is on the order of 10^{16} photons/cm^2-sec. The photolysis lamp output for the cell is monitored by a phototransistor, which can be used as a reference to detect fluctuations in the lamp intensities. The photolysis lamps are driven by a regulated power supply which can electronically switch them on and off in response to a reference square wave from a crystal oscillator.

The electronics for the instrument are designed to detect the periodic concentration fluctuations in the absorbing gases in the cell which are induced by the flashing of the photolysis lamps. This is done by two sequential stages of demodulation. The 400 cps AC signal from the detector carries the modulation information on sidebands at 400±f cps, where f is the frequency of the flashing lamps. The first demodulation is carried out by a 400 cps lock-in amplifier which produces a DC signal directly proportional to the spectroscopic light intensity. Riding on this DC signal as a low frequency ripple is the modulation information.

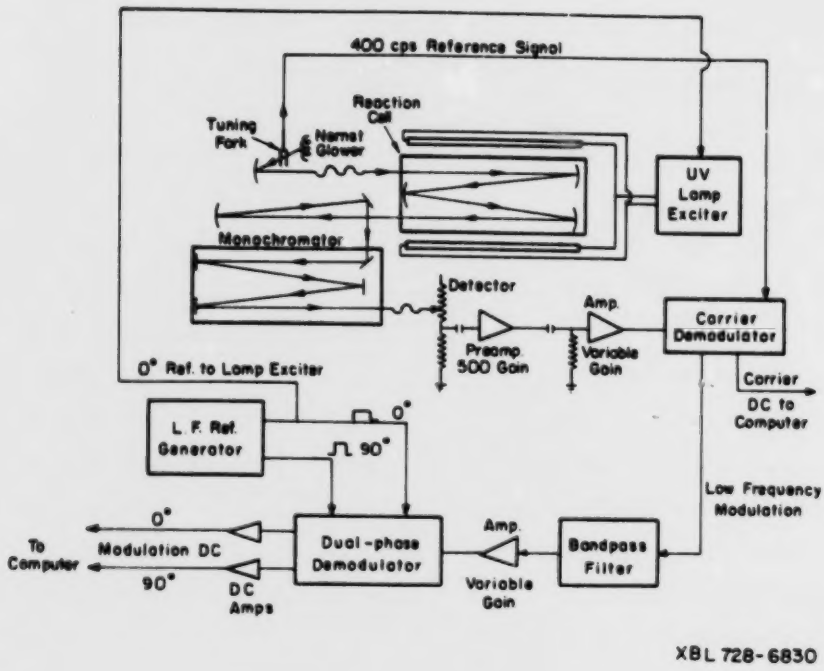

Figure 1 - Schematic diagram of experimental system with infrared detection of intermediates.

FIGURE 1

This DC signal is split in two with one component being recorded while the other is AC coupled, filtered, and sent into the second stage of demodulation. The second stage demodulator is a set of two lock-ins, operating at frequency f, with one lock-in reference in phase with the photolysis lamps and one reference exactly 90° out of phase. The outputs of these two lock-ins represent the amplitude of the sine and cosine components of the first fundamental of the modulation signal. From these values the phase shift and amplitude of the modulation signal can be calculated. The output of all three lock-in amplifiers are recorded and time averaged in a signal averaging computer.

B. ULTRAVIOLET APPARATUS

The basic system is analogous to that used in the infrared, although several new features were developed, especially the digital lock-in system. The reaction cell is a quartz cylinder 1.8 m long and 15 cm i.d. with a single mirror at one end. Two photolysis lamps were mounted outside the cell and backed by Alzak aluminum reflectors. The spectrometric light over the region 2000-3500 A is provided by a deuterium lamp (Bausch and Lomb DE-50A) powered by a well-stabilized power supply. A tuning fork (American Time Products) operating at 400 Hz chops the spectrometric beam at the cell entrance. The fork also provides a 400-Hz reference used in the detection system. A McPherson (Model 218, 0.3 m) monochromator equipped with a 2400-line/mm grating follows the reaction cell. An EMI photomultiplier (9526B) is mounted at the exit slit of the monochromator.

The output of the photomultiplier and the 400-Hz reference from the tuning fork are fed into a 400-Hz lock-in amplifier which separates the magnitude of the spectrometric light and the low-frequency modulation signal. A crystal oscillator is scaled down to control the photolysis lamps and to provide reference signals to compare with the modulated signal. The signal and references are sent to a digital lock-in where long-time averaging is obtained by means of reversible counters. The magnitude of the in-phase and 90° lag components is digitalized and punched into paper tape. This tape is later fed into a computer which

calculates phase shift and modulation amplitude at each wavelength of the spectrometric light.

The intensity of the photolyzing ultraviolet light was found by following the rate of decay of NO_2. This method requires exact values of the absorption coefficient of NO_2 as a function of wavelength (2700-4400A), quantum yield over the same range of wavelength, the spectral distribution of the photolyzing fluorescent lamp, and the full set of rate constants for the elementary reactions in this system (involving NO_2, NO, O, O_2, O_3, NO_3, and N_2O_5). To calculate the rate of production of Cl, it was necessary to combine the above data with the absorption coefficient of Cl_2 over the same range of wavelengths.[2]

In the infrared apparatus the average ultraviolet light intensity was 8.5×10^{15} photons/cm^2-sec), and the cross section for light absorption by chlorine weighted by the spectral distribution of the lamps used was 0.935×10^{-19} cm^2. Thus the rate of destruction of chlorine molecules is

$$d \ln[Cl_2]/dt = aI_o = 0.80 \times 10^{-3} \text{ sec}^{-1}$$

In the ultraviolet apparatus the photolyzing intensity is larger because two lamps are used and the cell has a small diameter.

$$I_o = 4.2 \times 10^{16} \text{ photons/(cm}^2 \text{ sec)}$$

$$aI_o = 3.92 \times 10^{-3} \text{ sec}^{-1}$$

C. MASS SPECTROMETER

A schematic diagram of the apparatus is shown in Figure 2. The photolyzing light was a 500 watt mercury arc lamp, filtered by Corning 9863 and 0160 filters immersed in a heat-removing solution of 0.1 M $CuSO_4$, passing a band between 3200 and 3800 Å. A rotating disk chopped the beam to give a square-wave photolyzing beam in the reaction cell. The chopper blade was driven by a Bodine synchronous motor coupled with a multiratio gear box to provide six different periods of rotation, 1, 2,

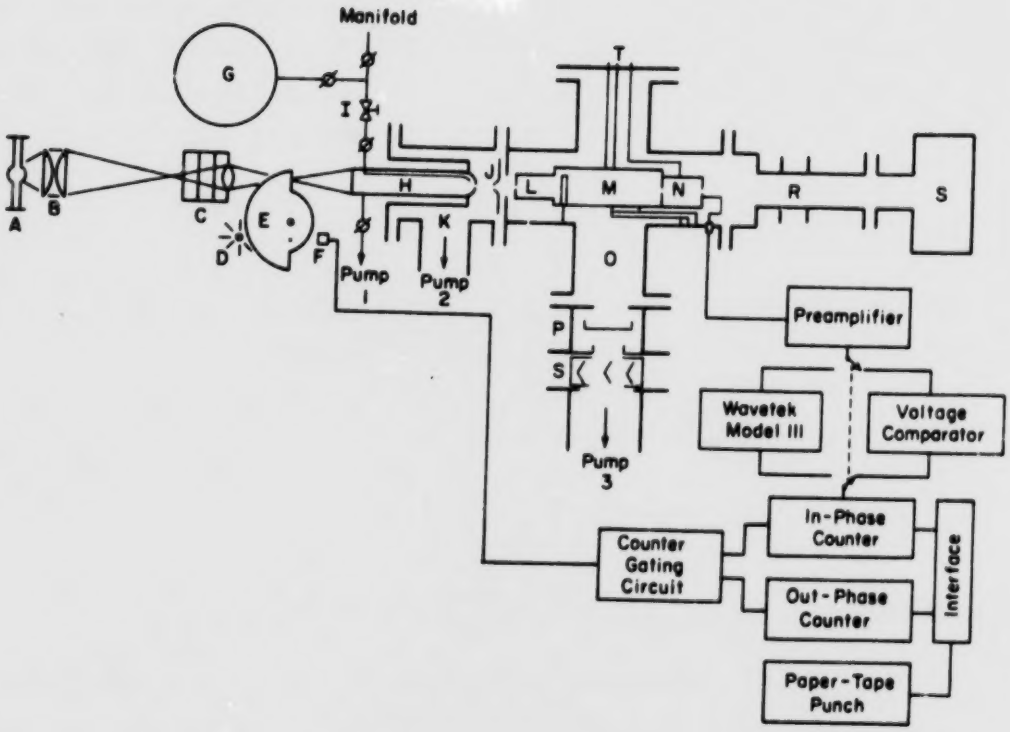

Figure 2 - Schematic diagram of the system using the mass spectrometer.

4, 8, 16 and 32 sec/cycle. A reference signal was provided by a small projector light and a photo-transistor placed on the opposite side of the blade from the photolyzing beam. The reaction cell (98 cc volume) was constructed of Pyrex with a quartz window fused on the rear through a graded seal. The front end was hemispherical in shape with a pin hole 33 μm in diameter to allow reaction gases to leak into the mass spectrometer. The pin hole was finished by grinding with a tapered copper rod to give a short, round, flared exit. After the gases left the reaction cell via the pin hole leak, they spread into an intermediate vacuum chamber, and a small portion intersected a "skimmer" to enter the high vacuum chamber of the mass spectrometer as a molecular beam. The size of the skimmer hole, angles of its opening, and its distance from the pin hole of the reaction cell were designed[11] to optimize the beam intensity and to avoid standing shock waves from blocking the entrance to the mass spectrometer. The intermediate chamber was evacuated by a Welch 1402B mechanical pump, NRC-4-SP type 121 diffusion pump, and a liquid nitrogen trap; during experiments its steady state pressure was just below 10^{-4} torr. The main chamber of the mass spectrometer was evacuated by a Marvac IDR2 mechanical pump, a 6 inch ultra-high vacuum CVC diffusion pump including water cooled chevron baffles and type TSMU sorbent trap. Also, a type PDV-2 ion pump was installed, but it was not operated during experiments because it introduced a substantial amount of noise to the electron multiplier. During experiments the chamber pressure was below 6×10^{-7} torr.

The mass spectrometer was of the quadrupole type, Extra-nuclear Laboratories, model 324, with a type II high efficiency electron-impact ionizer. Because of serious attack on the tungsten filament by chlorine and oxygen, it was replaced by a rhenium wire; 0.018 cm diameter. Six holes, 0.25 cm diameter, were drilled around the filament shield case to increase pumping speed in the ionization zone. The system was aligned so that the pin hole, the skimmer, the ionization zone, and the axis of the mass spectrometer were all in a straight line. Ions were detected by an electron multiplier, closely coupled to a bakeable preamplifier with 10^7 ohm input resistance, which gave a frequency response from DC to 100 kHz.

In the reaction cell, reactants and products were present typically in amounts 4 to 6 orders of magnitude higher than free radical intermediates. To cover this very wide range, we measured free radicals by a direct ion counting technique, and reactants by analogue, current measuring methods[5] Circuit constants were such that the ion counting method was useful for constituents in the reaction cell between 10^{10} and 10^{15} molecules/cc, and the analogue method was useful from 10^{14} to 10^{18} molecules/cc. An ion event was amplified by the electron multiplier to give a pulse in the preamplifier. The pulses were passed into a voltage comparator that rejected as noise pulses below a certain level and sent higher pulses into a "one shot" circuit, which converted them to a uniform height of 4 volts and a uniform width of 5 μsec. The complete period, T, of a cycle of photolysis, light and dark portions, was precisely divided into 4 equal parts: O to T/4 (light on), T/4 to T/2 (light on), T/2 to 3 T/4 (light off), 3 T/4 to T (light off). Pulses from the "one shot" circuit were passed to two Hewlett-Packard model H19-5280 A reversible counters, one adding from 0 to T/2 and subtracting from T/2 to T, called the in-phase counter and the other adding from T/4 to 3T/4 and subtracting during the other intervals, called the out-phase counter. To record the mass spectrum at a given number, a large number of cycles of photolysis was accumulated in the counters. It is very important to have the time for counting positively to be exactly equal to the time of negative counting; otherwise unbalanced counts will accumulate after many cycles. The timing system has an accuracy of one part per million for 30 seconds of averaging time. After completing a pre-set number of complete cycles, the counting stopped, and the net counts from each counter were puched out on paper tape. Later the paper tape was fed into a computer, which calculated the desired functions. Analogue signals were processed and recorded by the method of Morris and Johnston[8].

SECTION V

NATURE OF RESULTS

A. SIMPLE GRAPHICAL PRESENTATION

The effect of intermittent ultraviolet illumination upon a photolabile chemical system is to bring about, through photolytic decomposition of one of the reactants, a periodic variation in its concentration and that of the intermediates directly formed. Ensuing reactions bring about fluctuations in the concentrations of other intermediates and products, as well. Use of a well-stirred continuous-flow reaction vessel permits experimental measurements to be made under quasi-steady-state conditions: the concentrations of the various species fluctuate about average values which remain constant with time, and spatial concentration gradients are negligible. Concentrations fluctuations modulate the amplitude of the 400 cps IR beam transmitted through the reaction vessel giving rise to an amplitude-modulated electrical signal from the IR detector.

Although the frequency of the molecular modulation coincides with the frequency of pulsed ultraviolet illumination, it is, in general, displaced in phase from the ultraviolet excitation voltage. The extent of the phase shift depends upon whether the modulation is due to a reactant, intermediate or product, and also upon the lifetime of the absorber under the conditions of the reaction, relative to the period of ultraviolet illumination. Since we are ultimately concerned with determining the lifetimes of some of the chemical species involved, as well as their identities, measurement of the phase shift is a means of obtaining the former information and very often the latter as well.

The output of the dual phase demodulator consists of two D.C. voltages which permit the evaluation of the phase shift in the following manner. The input signal to the dual phase demodulator may be represented as:

$E = E_o \sin(2\pi\nu t + \delta)$ where E_o is a measure of amplitude of molecular modulation

ν = frequency of uv excitation

δ = phase shift between uv excitation and molecular modulation

The phase of the reference signal to the dual phase demodulator may be varied over a considerable range in each channel, but as a rule, it is adjusted so that it is exactly in or out-of-phase with the ultraviolet excitation in channel A, and 90° leading or lagging with respect to the ultraviolet in channel B. Therefore, the D.C. output voltages of channels A and B, respectively, are, after detection and filtering out the second harmonic:

$$E_A = E(E_{REF})_A = E_o \sin(2\pi\nu t + \delta) \sin 2\pi\nu t$$

$$= (E_o/2) \cos \delta, \text{ for channel A in-phase}$$

$$E_B = E(E_{REF})_B = E_o \sin(2\pi\nu t + \delta) \cos 2\pi\nu t$$

$$= (E_o/2) \sin \delta, \text{ for channel B 90°-leading}$$

Combination of these equations yields the following relationships for the phase shift and amplitude of the molecular modulation signal:

$$\delta = \text{Arctan}\ (E_B/E_A)$$

$$E_o = 2(E_A^2 + E_B^2)^{1/2}$$

The extent of the phase shift δ in the modulated IR signal is a function of the species involved and its lifetime relative to the period of the ultraviolet illumination.

For a reliable quantitative evaluation of the lifetimes, it is necessary that the phase shift be made to assume some value removed from 0, 90, 180 or 270° with respect to the ultraviolet light. This is accomplished either by varying reaction conditions, or the rate of pulsing the ultraviolet light, or both. One can then obtain the lifetime from the

measured phase shift and the ultraviolet flashing frequency alone, or in conjunction with the dependence of the signal amplitude upon flashing frequency of the ultraviolet lamp.

In general, the identity of an absorber responsible for a given modulation signal can be ascertained from the shape and position of its absorption spectrum. However, if this is not possible due to either overlap of absorption bands of several species in the reaction or to the fact that the absorption spectrum is not known, then the species can often be identified as a reactant, intermediate or product by the phase shift. The principles involved will be illustrated by three hypothetical reactions.

PRIMARY PHOTOCHEMICAL REACTION

If reactant A absorbs light directly to form product C, without formation of intermediate species, the mechanism is

$$A + h\nu \rightarrow C + \ldots$$

The exciting light is electrically switched on and off to produce a square wave, Figure 3. When the light is on, reactant A decreases and product C increases; when the light is off, both A and C remain constant, Figure 3. If each of the three periodic functions of Figure 3 is resolved into its fundamental A.C. component, it is found that the reactant leads the photochemical light by 90° (phase shift of +90° or of -270°), and the product lags behind the photolysis light by 90° (phase shift of -90°). The reactants and products as shown in Figure 3 are as they would appear in a static gaseous system, with a steady decrease of reactant and build-up of product. In our actual system, the reactant and carrier gases flow rapidly through the cell, so that the combination of stirred-flow and photochemical processes yields reactant and product concentrations that fluctuate about a steady-state value; the phase relationships shown in Figure 3 are preserved in this case.

PHOTOCHEMICAL PROCESS WITH FORMATION OF INTERMEDIATE

The mechanism in this case is simply

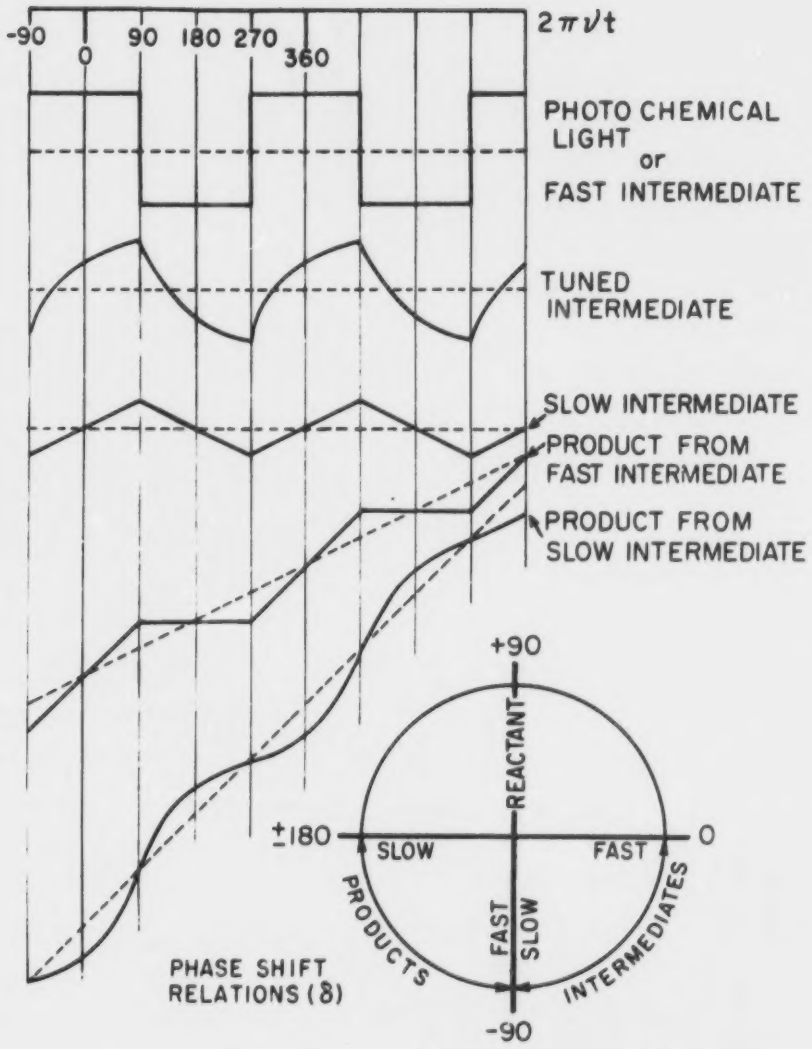

Figure 3 - Phase relations between photolysis light, reactant, and product of a primary photochemical reaction (in static, non-flowing system).

$$A + h\nu \rightarrow X+\cdots$$
$$X+ \rightarrow C+\cdots$$

Where X is an intermediate (usually, but not necessarily, a free radical). If the reactant is neither regenerated by the intermediate X nor attacked by X, then its phase relationship is the same as that of Figure 3. The phase relationship of intermediate X to photochemical light varies, depending on the relationship between duration of light flash and the lifetime of the intermediate in the system, as shown in Figure 4. Three cases of intermediates are shown: (1) Fast intermediate. The lifetime of the intermediate is very short compared to duration of light, and in this case the intermediate concentration is proportional to light intensity at all times, with a zero phase shift. (2) Slow intermediate. The lifetime of the intermediate is very long compared to duration of light pulse; the intermediate continues to build up throughout the light period and continues to decay after the light turns off. After an induction period the intermediate oscillates with a triangular wave form about a steady state value, with a low A.C. amplitude and a 90° phase shift. (3) Tuned intermediate. The lifetime of the intermediate is about the same as the duration of the light; for the case shown in Figure 4, the half-life of the intermediate is one-fourth of the duration of the light-on period. The phase-shift of the product depends on the phase-shift of the intermediate. As can be seen from Figure 4, a product arising from a "fast intermediate" has a phase-shift of -90°, and a product arising from a "slow intermediate" has a phase-shift of -180°. For a "tuned intermediate", the intermediate itself will have a phase-shift between 0° and -90°, and the product will have a phase-shift between -90° and -180°.

COMPLEX PHOTOCHEMICAL REACTIONS

For any mechanism of interest, the expected phase-shifts can be derived from graphical constructions, such as Figure 3 or Figure 4. However, for complex systems it becomes more convenient to treat the case analytically, in terms of a system of simultaneous differential equations, or numerically on a computer. Results of such an analysis for a simple

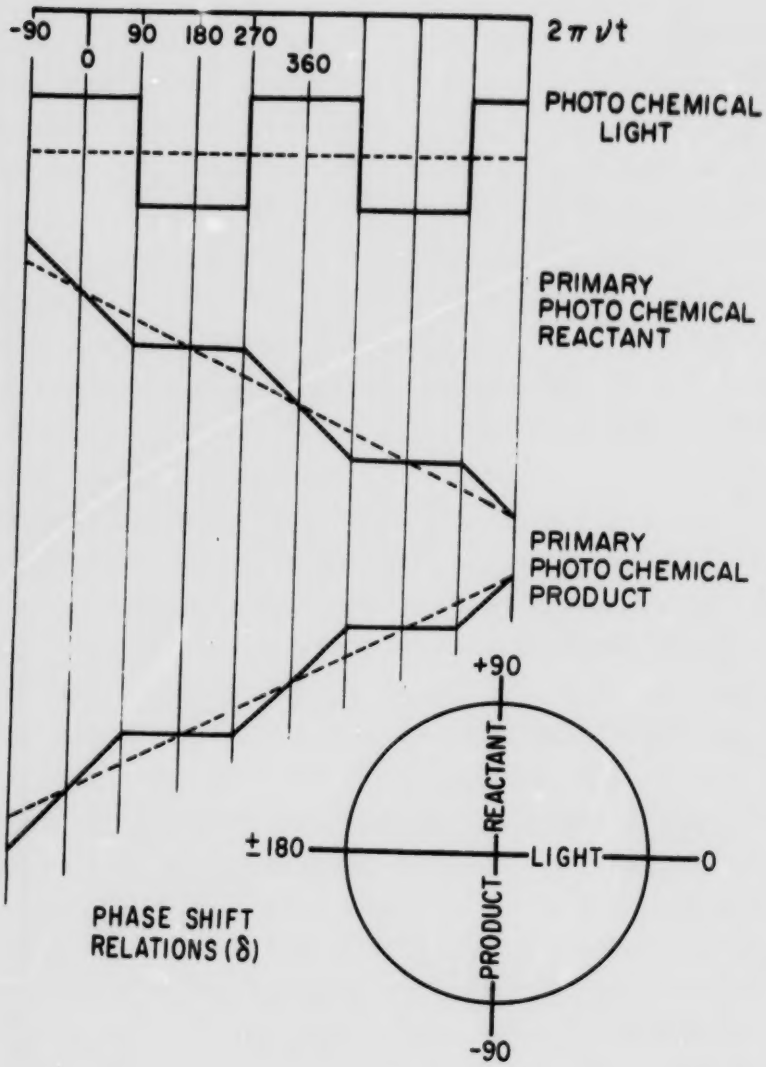

Figure 4 - Photochemical reaction with simple, single intermediate (non-flowing system).

general mechanism is given here. The mechanism is:

$A + h\nu \rightarrow X + Y$	$R_1 = k_1 I_o[A]$
$X + Y \overset{(M)}{\rightarrow} A$	$R_2 = k_2(M)\ [X]\ [Y]$
$X + A \rightarrow$ products	$R_3 = k_3[X]\ [A]$
(other reactions not involving A)	
Change of species S by virtue of flow through reactor	$F_s = (f/V\ ([S]-[S]_o)$

where R's are rates, k's are rate constants, f is volumetric flow rate and V is volume of reactor, subscript zero refers in concentration of species as it flows into the reactor. The reactant A is destroyed photochemically, regenerated by recombination of radicals, and destroyed by radicals. The total range of phase shifts for this example is given by Figure 5. Intermediates can have a phase shift between 0 and -90°; products can have a phase shift between -90° and -180°. So long as reactants, intermediates, and products have separate wave-length regions of optical absorption, this method gives kinetic information: life-times of all intermediates, spectra of intermediates, a direct clue as to the radical precursors of various products, and a direct clue as to the interaction of radicals with reactants.

It should be noted that this method gives only the change in reactant or product concentration per cycle, and thus the signals from reactants and intermediates are the same order of magnitude, even though reactants may exceed intermediates by a factor of a million or more.

B. MATHEMATICAL BASIS FOR THE METHOD

The reaction scheme below illustrates the important types of chemical species in a modulation experiment. The species A through F are stable molecules; and X, Y, and Z are free radicals. The modulation of each species is a function of the type of species and of the elementary

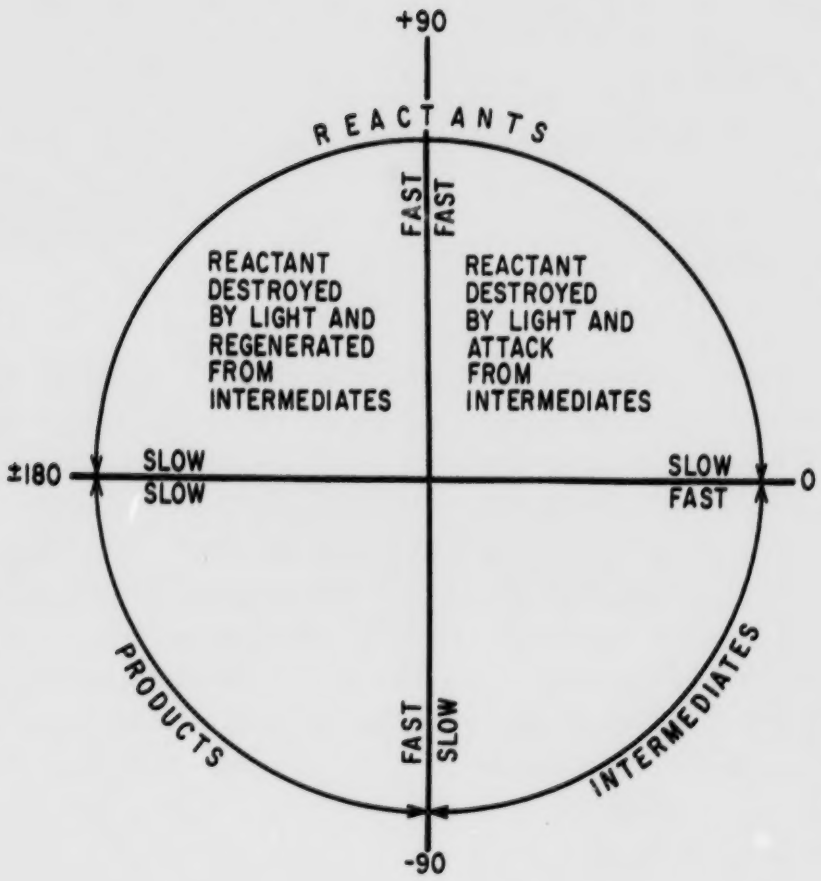

Figure 5 - Phase relations between photolysis light, reactants, intermediates, and products in complex photochemical reaction.

$$A + h\nu \rightarrow 2X \quad (1)$$

$$X + B \xrightarrow{k_1} Y + C \quad (2)$$

$$Y + D \xrightarrow{k_2} Z + E \quad (3)$$

$$Z + Z \xrightarrow{k_3} F \quad (4)$$

Since the concentrations of the species in the chemical system vary periodically in time, they can be represented by a Fourier expansion of the form

$$f(\omega t) = \sum_n [a_n \sin(n\omega t) + b_n \cos(n\omega t)] + b_o$$

where ω is the fundamental angular frequency of the wave obtained from the period T by the relation $\omega = 2\pi/T$. An alternative form of the Fourier expansion is:

$$f(\omega t) = \sum_n c_n \sin(n\omega t + \delta_n) + c_o.$$

The two are related by:

$$c_n = (a_n^2 + b_n^2)^{1/2} \text{ and } \delta_n = \tan^{-1}(b_n/a_n).$$

The coefficients c_n are amplitudes; the quantities δ_n are phase shifts. In the following analysis, the photolytic lamp is represented by an expansion involving sine terms only, i.e., all $b_n = 0$. Hence all $\delta_n = 0$. For any chemical species, then, δ_n is its phase shift relative to the photolytic lamp.

REACTANT DECOMPOSED BY LIGHT

The differential equation for A is:

$$\frac{d[A]}{dt} = \frac{f'}{V}[A]_o - \sigma[A]\frac{I_o}{2} + \frac{2I_o}{\pi}\sum_n, \text{ odd } \frac{1}{n}\sin(n\omega t) - \frac{f'}{V}[A] \quad (5)$$

where f' is the flow rate into and out of the cell in liters/sec.

V is the volume of the cell in liters

$[A]_o$ is the concentration of A entering the cell in molecules/cm^3

I_o is the photon flux in photons/cm^2.sec

σ is the absorption cross-section of the reactant in cm^2/molecule

[A] is the concentration of A

ω is the flashing frequency in radians/sec

t is the time in sec

Since $\omega = 2\pi/T = 2\pi f$ where f is the flashing frequency in cycles/sec., we can write $\theta = \omega t = 2\pi f t$ from which we get $d\theta/dt = 2\pi f$ or $dt = d\theta/2\pi f$, giving

$$\frac{d[A]}{d} = \frac{1}{2\pi f}\left(\frac{f'}{V}[A]_o - \sigma[A]\frac{I_o}{2} + \frac{2I_o}{\pi}\sum_n, \text{ odd } \frac{1}{n}\sin(n\theta) - \frac{f'}{V}[A]\right) \quad (6)$$

When the change in concentration over a flashing period is small compared to the total concentration ($\Delta[A] < 10^{-2}[A]$), [A] on the right side of the differential equation may be regarded as a constant. Collecting the D.C. terms we have

$$\frac{d[A]}{d\theta} = \frac{1}{2\pi f}\left(\frac{f'}{V}[A]_o - \left(\frac{\sigma I_o}{2} + \frac{f'}{V}\right)[A] - \frac{2\sigma I_o[A]}{\pi}\sum_n, \text{ odd } \frac{1}{n}\sin(n\theta)\right).$$

The requirement of a stable D.C. concentration means

$$\left(\frac{f'}{V}[A]_o - \left(\frac{\sigma I_o}{2} + \frac{f'}{V}\right)[A] = 0\right.$$

which gives the following simplified differential equation

$$\frac{d[A]}{d\theta} = -\frac{2\sigma I_o[A]}{2\pi^2 f}\sum_n, \text{ odd } \frac{1}{n}\sin(n\theta).$$

As long as the concentration modulation, $\Delta[A]$, is much smaller than the total concentration, [A], the equation is linear and is easily integrated[12] giving the concentration modulation

$$[A]_{mod} = \frac{\sigma I_o[A]}{\pi^2 f}\sum_n, \text{ odd } \frac{1}{n^2}\cos(n\theta). \quad (7)$$

From the definition of phase shift, we see that the reactant concentration modulation has a phase shift of +90° with respect to the flashing lamp. The modulation of A is seen to be a triangular wave whose amplitude is inversely proportional to the flashing frequency.

RADICAL FORMED BY THE INITIAL PHOTO-DISSOCIATIVE STEP AND DECAYING BY A PROCESS FIRST-ORDER IN RADICAL CONCENTRATION

The differential equation describing the radical concentration [X] in terms of the previously defined quantities σ, [A], ω, and I_o and the concentration of reactant B, is:

$$\frac{d[X]}{dt} = 2\sigma[A]\left(\frac{I_o}{2} + \frac{2I_o}{\pi}\sum_{n,\ \text{odd}}\frac{1}{n}\sin(n\omega t)\right) - k_1[B]\,[X]. \qquad (8)$$

This can be solved in a straight forward manner like the previous case to yield:

$$[X] = \frac{2\sigma I_o[A]}{\pi^2 f}\sum_{n,\ \text{odd}}\left(\frac{k_1[B]}{2\pi f}\frac{1}{n}\sin(n\theta) - \cos(n\theta)\right)\Big/\left(\left(\frac{k_1}{2}\frac{[B]}{\pi f}\right)^2 + n^2\right)$$

$$+ \frac{\sigma I_o[A]}{k_1[B]}. \qquad (9)$$

When this equation for [X], the radical concentrations, is taken to its low frequency limit we get:

$$\lim_{f\to 0}[X] = \frac{4\sigma I_o[A]}{\pi k_1[B]}\sum_{n,\ \text{odd}}\frac{1}{n}\sin(n\theta) + \frac{\sigma I_o[A]}{k_1[B]}. \qquad (10)$$

This is the equation of a square wave with an amplitude of $\sigma I_o[A]/k_1[B]$ oscillating about a D.C. level of $I_o[A]/k_1[B]$. Thus the radical concentration has a maximum of $2\sigma I_o[A]/k_1[B]$-- the radical concentrations one obtains from the "steady-state" approximation for [X]. Note also that the phase shift of the radical concentration is 0°. At high frequencies we have:

$$\lim_{f\to\infty}[X] = \frac{2\sigma I_o[A]}{\pi^2 f}\sum_{n,\ \text{odd}} -\frac{1}{n^2}\cos(n\theta) + \frac{\sigma I_o[A]}{k_1[B]} \qquad (11)$$

So [X] becomes a triangular wave with vanishing amplitude oscillating about a D.C. level equal to one-half the "steady-state" concentration. The phase shift is -90°.

It is convenient to define the "life-time" of the radical, X, to be

$$\tau_1 = \frac{1}{k_1 B}$$

which is the time required for the concentration to drop by a factor of e. The behavior of the fundamental of [X] at intermediate flashing frequencies is plotted in Figure 6 as a function of the ratio of the flashing period (T=1/f) to the radical life-time.

The phase shift of the fundamental of [X] is given by:

$$\delta = \tan^{-1} (b_1/a_1) = \tan^{-1} (-1/(k_1[B]/2\pi f)).$$

So

$$k_1[B] = \frac{-2\pi f}{\tan\delta} .$$

Thus the radical life-time can be found from just one phase shift measurement at one frequency if the radical species is known to be formed in the initial step and to decay by a process first-order in radical concentration.

RADICAL FORMED BY A RADICAL-MOLECULE REACTION AND DECAYING BY A PROCESS FIRST-ORDER IN RADICAL CONCENTRATION

When a radical is formed by the reaction of a preceding radical, X, with a molecule, B, and is destroyed by reaction with another molecule, D, the differential equation describing the concentration of the new radical, Y, is:

$$\frac{d[Y]}{dt} = k_1[B]\ [X] - k_2[D]\ [Y]. \qquad (12)$$

Integration of this equation after changing the variable from t to θ

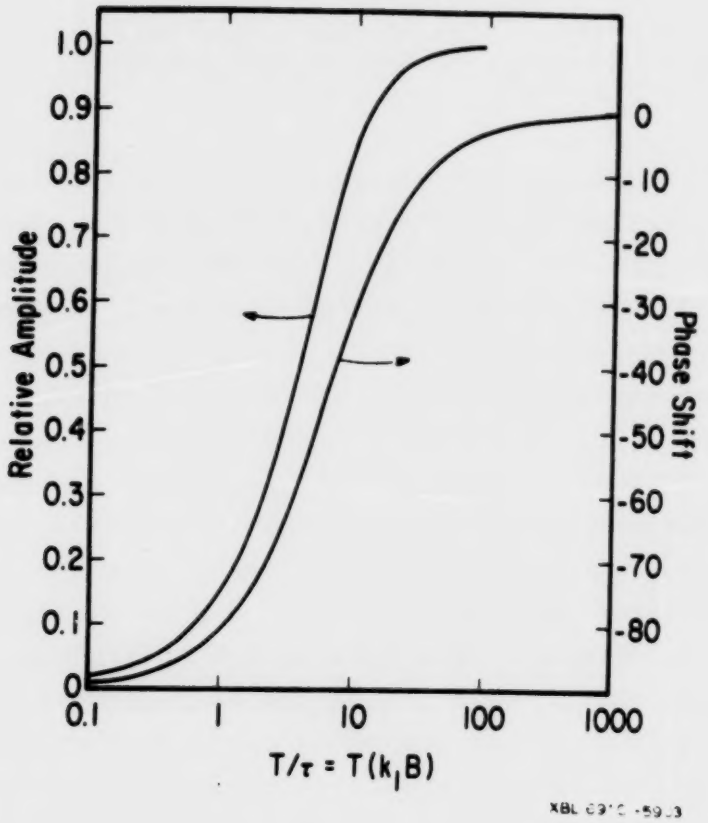

Figure 6 - Dependence of the fundamental modulation frequency of a primary first-order radical on the ratio of flashing period to radical life-time. The amplitude is relative to the limiting amplitude as T/τ approaches infinity.

and substituting Eq. (9) for [X] gives

$$[Y] = \frac{\sigma I_o[A]}{k_2[D]} + \frac{2\sigma I_o[A]}{\pi^2 f}\frac{k_1[B]}{2\pi f}\sum_n, \text{ odd } \left(\frac{k_1[B]k_2[D] - (2\pi fn)^2}{(2\pi f)^2 n^2\left((k_1[B]/2\pi f)^2 + n^2\right)} \sin(n\theta) \right.$$

$$\left. - \frac{k_2[D] + k_1[B]}{2\pi f\left((k_1[B]/2\pi f)^2 + n^2\right)} \cos(n\theta) \right) / \left((k_2[D]/2\pi f)^2 + n^2 \right). \qquad (13)$$

Since the coefficients b_n are always negative and the coefficients a_n may be either positive or negative depending on the sign of $k_1[B]k_2[D] - (2\pi fn)^2$, the phase shift of the fundamental of [Y] may lie anywhere between 0° and -180°. The dependence of the concentration modulation of Y on flashing frequency is determined by $k_1[B]$, $k_2[D]$, and f. A convenient way of looking at the modulation of Y is to plot the amplitude and phase shift of the fundamental as a function of T/τ_1 for several values of τ_2/τ_1. This is done in Figure 7 and 8. When τ_2/τ_1 is large, at frequencies where the primary radical X has a phase shift close to 0°, the secondary radical Y behaves like a primary radical. Under such conditions the life-time of Y can be easily obtained. When τ_2/τ_1 is small, however, determination of the life-time will be difficult because the phase shift of the secondary radical Y is determined, for the most part, by the phase shift of the preceding radical. At flashing frequencies high enough to impart a substantial phase shift to the secondary radical due to its own inherent life-time, the modulation amplitude of the preceding radical is very low. As a result, the modulation amplitude of the secondary radical is also very small making detection difficult.

RADICAL WHICH DECAYS BY A PROCESS SECOND-ORDER IN RADICAL CONCENTRATION

The differential equation for the second-order radical Z is

$$\frac{d[Z]}{dt} = k_2[D][Y] - 2k_3[Z]^2. \qquad (14)$$

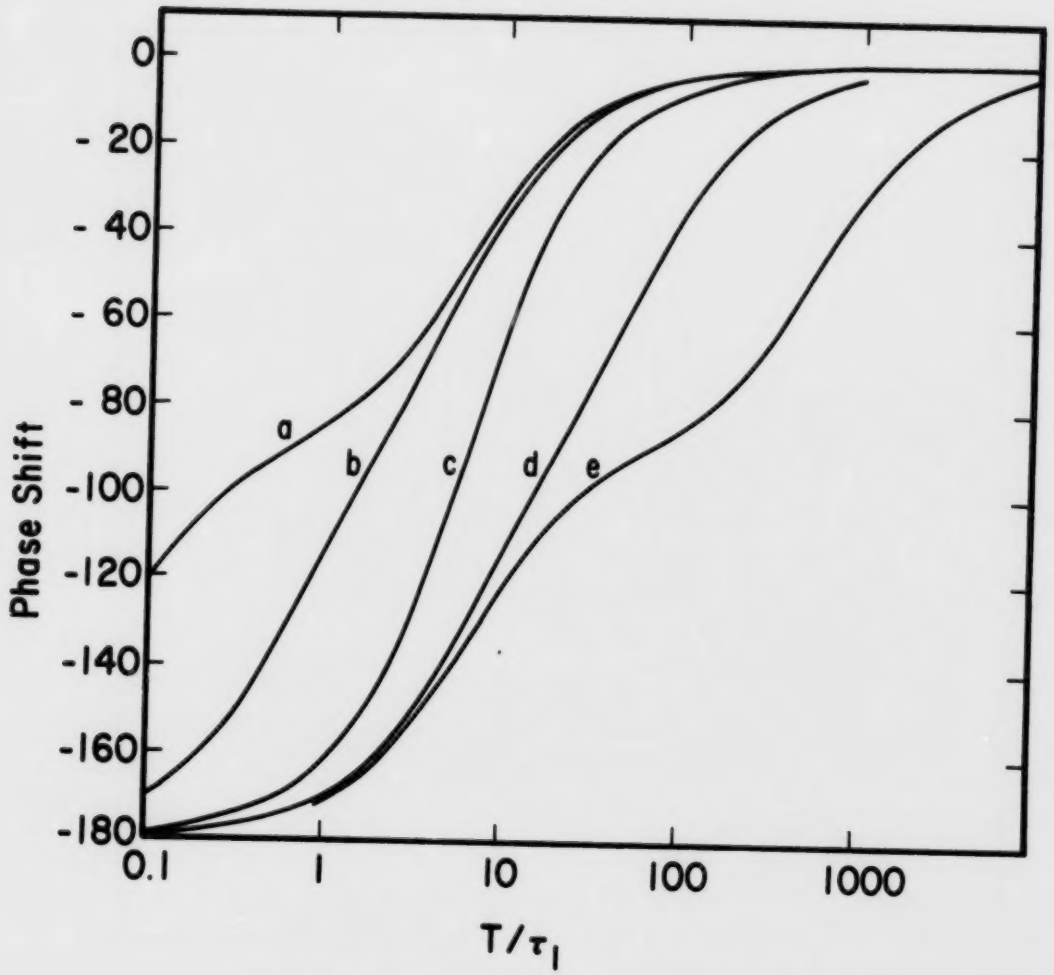

XBL 6910-5905

Figure 7 - The dependence of the modulation of a secondary radical on the ratio of its life-time to the life-time of the preceding radical. a) $\tau_2/\tau_1 = 0.01$; b) $\tau_2/\tau_1 = 0.10$; c) $\tau_2/\tau_1 = 1.00$; d) $\tau_2/\tau_1 = 10$; e) $\tau_2/\tau_1 = 100$.

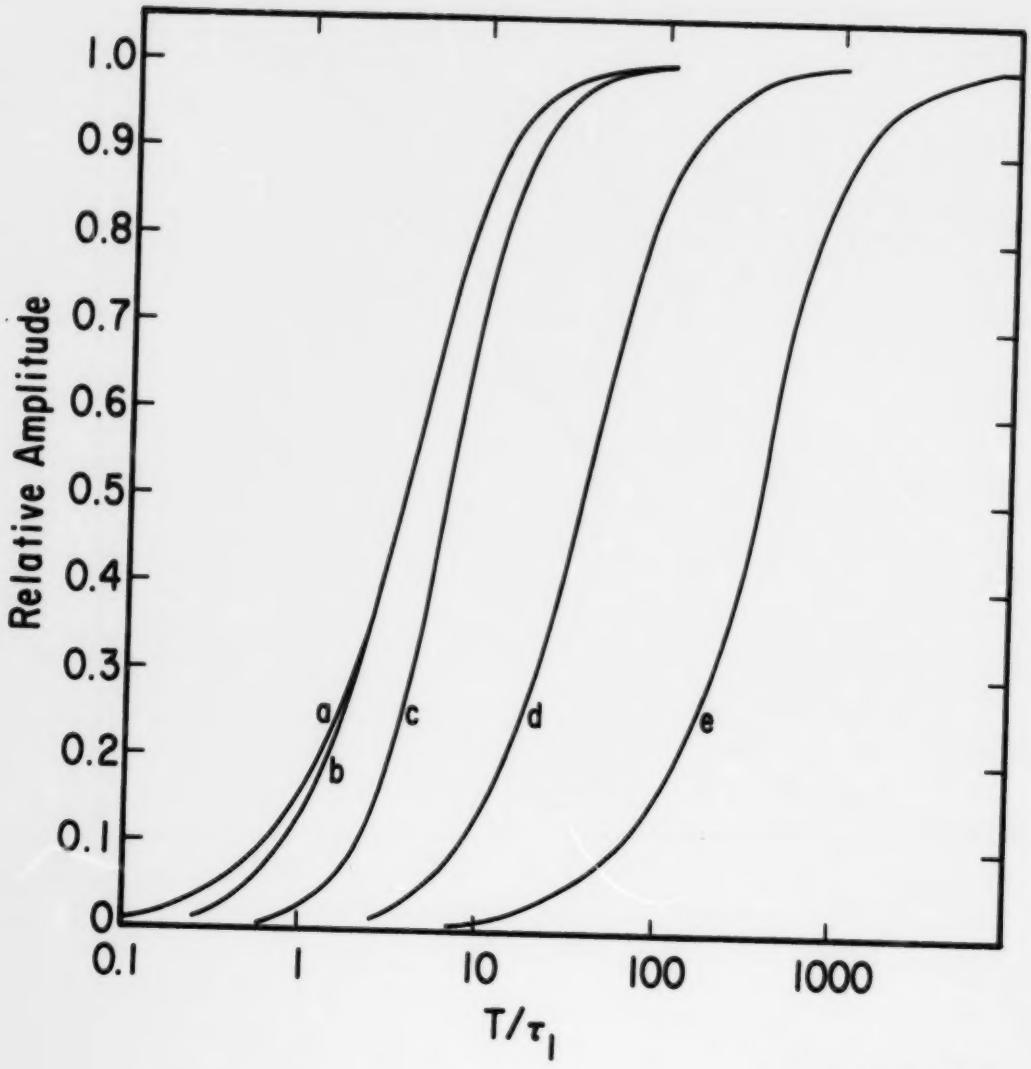

XBL 6910-5907

Figure 8 - Modulation amplitude relative to the limiting amplitude as T/τ_1 approaches infinity. a) $\tau_2/\tau_1 = 0.01$; b) $\tau_2/\tau_1 = 0.10$; c) $\tau_2/\tau_1 = 1.00$; d) $\tau_2/\tau_1 = 10$; e) $\tau_2/\tau_1 = 100$.

This equation is intractable because the equation is non-linear, and [Y] and [Z] are both functions of t. A special case of (14) is of considerable interest

$$\frac{d[Z]}{dt} = P - Q[Z]^2 \tag{15}$$

where P and Q are constant. This case can arise from (14) if the radical Y is very fast and is in phase with the exciting light. Another case occurs when the radical Z is formed directly from the primary photolysis of the reactant. A numerical solution to (14) can be readily obtained if the equation is written in two parts, one corresponding to the lamp on and one to the lamp off.

$$\frac{d[Z]}{d\theta} = \frac{1}{2\pi f}\left(P - Q[Z]^2 \right) \quad -\pi \leq \theta \leq 0 \tag{16}$$

$$\frac{d[Z]}{d\theta} = -\frac{1}{2\pi f} Q[Z]^2 \qquad 0 \leq \theta \leq \pi \tag{17}$$

Each of these equations can be integrated; the solution with the lamp on is

$$[Z]_\theta = \left(\frac{P}{Q} \right)^{\frac{1}{2}} \tanh \frac{(\theta+\pi)\,(PQ)^{\frac{1}{2}}}{2\pi f} \tan^{-1} \frac{[Z]_{-\pi}}{(P/Q)^{\frac{1}{2}}}$$

and with the lamp off it is

$$[Z]_\theta = \frac{2\pi f [Z]_0}{2\pi f + Q\theta [Z]_0}$$

Using these two equations, we may assume an initial value for $[Z]_{-\pi}$, calculate $[Z]_0$ and $[Z]_\pi$, set $[Z]_{-\pi} = [Z]_\pi$, and recalculate $[Z]_0$ and $[Z]_\pi$ until $[Z]_\pi = [Z]_{-\tau}$ within a desired degree of accuracy. Having found $[Z]_{-\tau}$, we then calculate [Z] for small increments of θ (e.g., $\Delta\theta = 2\pi/100$). The resulting table of $[Z]_\theta$ vs. θ provides the basis for the Fourier analysis of [Z]. For the periodic function

$$[Z] = \sum a_n \sin(n\theta) + b_n \cos(n\theta) + b_o/2$$

the coefficients a_n and b_n can be found by the numerical integrations

$$a_n = \frac{1}{\pi} \sum_{i=1}^{m} [Z]_{\theta_i} \sin(n\theta_i)\Delta\theta$$

$$b_n = \frac{1}{\pi} \sum_{i=1}^{m} [Z]_{\theta_i} \cos(n\theta_i)\Delta\theta$$

where m is the number of increments of θ. Such an analysis has been done over a wide range of flashing frequencies. The amplitude and phase shift behavior of the fundamental as a function of the ratio of flashing period to radical life-time is shown in Figure 9. Because the life-time of a second-order species depends on concentration, we define "the radical life-time" to be the half-life of the radical from its steady-state concentration. The steady-state concentration of the radical Z is

$$[Z]_{ss} = \left(\frac{2\sigma I_o [A]}{2k_3}\right)^{\frac{1}{2}} = (P/Q)^{\frac{1}{2}} \qquad (18)$$

and the life-time becomes

$$\tau = \frac{1}{2k_3[Z]_{ss}} = (PQ)^{-\frac{1}{2}} \qquad (19)$$

Comparison of the life-time formulae for the first- and second-order radicals indicated how these kinetically different radicals can be distinguished experimentally. The life-time of a first-order radical, given by

$$\tau = 1/k_1[B], \qquad (20)$$

is independent of radical formation rate and inversely proportional to the concentration of a reactant involved in the radical's decay. The life-time of a second-order radical given by (19) is inversely proportional to the square-root of the radical formation rate. Changes in reactant concentration affect the life-time only be affecting the radical formation rate. Thus varying reactant concentrations and the

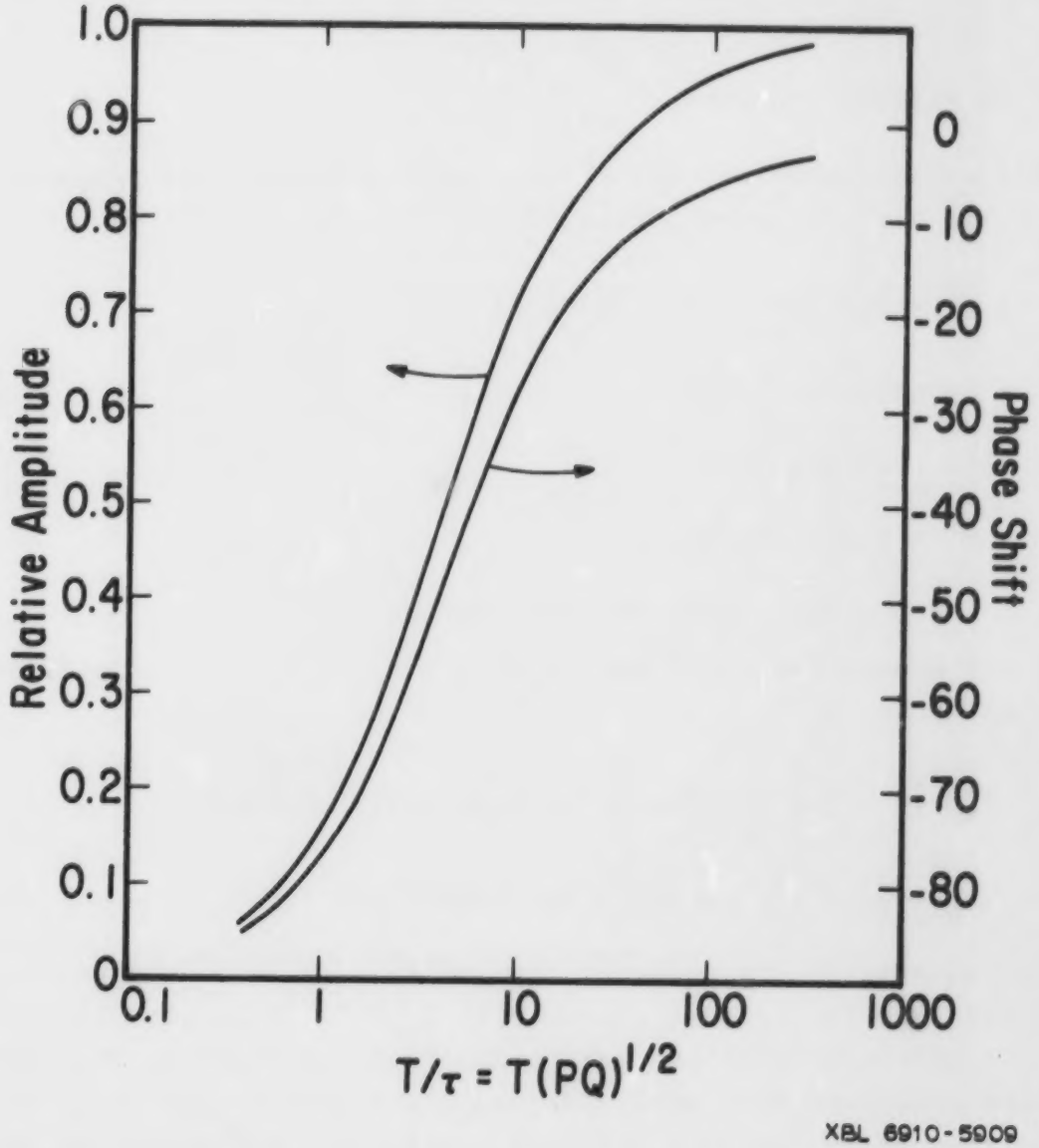

Figure 9 - Concentration modulation of a second-order radical as a function of the ratio of flashing period to radical lifetime. The amplitude is relative to the limiting amplitude as T/τ approaches infinity.

photolytic light intensity can provide the information necessary to determine whether the radical decay reaction is first or second order in radical concentration.

PRODUCT OF RADICAL REACTIONS

The differential equations describing the behavior of the products, C, E, and F all have the same general form:

$$\frac{dJ}{d\theta} = \frac{k'}{2\pi f}\left(G + H \sum \alpha_n \sin(n\theta) + \beta_n \cos(n\theta)\right) - \frac{f'}{V} J \qquad (21)$$

where $J = [C]$, $[E]$, or $[F]$

$k' = k_1[B]$, $k_2[D]$, or k_3

G = the D.C. level of $[X]$, $[Y]$, or $[Z]^2$

and H = the modulation amplitude of $[X]$, $[Y]$, or $[Z]^2$. The solution to this equation is

$$J = k'G\frac{V}{f'} + \frac{k'H}{2\pi f}\sum_{n,\ \text{odd}} \left\{ \left[\left(\alpha_n \frac{f'}{2\pi fV} - n\beta_n\right)\sin(n\theta) + \left(\beta_n \frac{f'}{2\pi fV} + \alpha_n\right)\cos(n\theta)\right] / \left[(f'/2\pi fV)^2 + n^2\right] \right\}. \qquad (22)$$

From this equation it is apparent that if $f'/2\pi fV \ll 1$, the product fundamental lags the radical fundamental by 90°. Note also the inverse dependence of the product modulation amplitude on flashing frequency. This means that a product amplitude falls off faster with increases in flashing frequency than does that for a radical. The amplitude and phase shift behavior of the product of a second-order radical is presented in Figure 10.

REACTANT ATTACKED BY A RADICAL

The differential equation for a reactant B which is attacked by a radical is of the same form as the equation in Section 5 with two minor

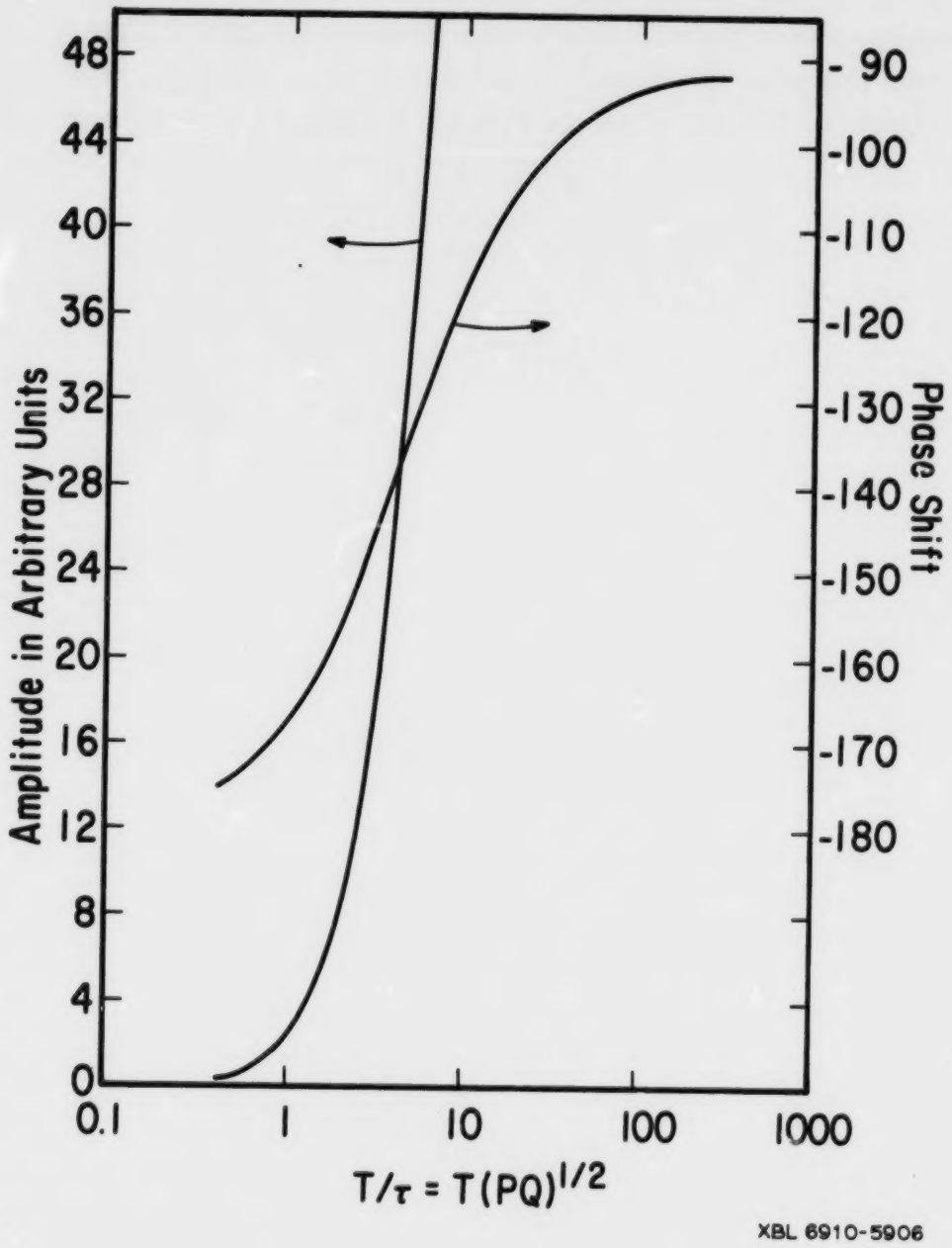

Figure 10 - Concentration modulation of the product of a second-order radical as a function of the ratio of the flashing period to life-time of the radical forming the product. Note the strong dependence of amplitude on T/τ.

differences: there is a flow-in term $(f'/V)\ [B]_o$) and a change in sign because molecules are being lost through reaction. The solution shows that the reactant modulation leads the radical by 90°. Also the reactant amplitude has the same frequency dependence as a product, i.e., it falls off faster than a radical with increases in flashing frequency.

SECTION VI

CHLORINE OXIDE RADICALS

A. INTRODUCTION

The ClOO radical was first proposed by Porter and Wright[13] as an intermediate in the flash photolysis of chlorine-oxygen mixtures.

$$Cl_2 + h\nu \longrightarrow Cl + Cl$$

$$Cl + O_2 + M \longrightarrow ClOO + M$$

$$Cl + ClOO \longrightarrow ClO + ClO$$

$$Cl + ClOO \longrightarrow Cl_2 + O_2$$

$$ClO + ClO \longrightarrow Cl_2 + O_2$$

From absorption spectroscopy in the ultraviolet (2600-3000 A) they observed the intermediate diatomic radical ClO. Although not observed, the peroxy radical was postulated to be a short lived precursor to ClO in their system. Since then, the ultraviolet absorption spectrum of ClO has been observed repeatedly,[14-24] however, until recently no spectrographic evidence existed for the presence of ClOO. Arkell and Schwager[25] published an infrared spectrum attributed to matrix-isolated ClOO. This system was chosen originally as a test case for the molecular-modulation method; but new, interesting results were obtained and the spectra of ClOO and ClO was explored by infrared, ultraviolet, and mass spectrometry.

B. INFRARED SPECTROSCOPIC MEASUREMENTS

Exploratory scans were carried out over a fairly wide spectral region. The region from 800 to 200 cm^{-1} was scanned using a 100-sec time constant. A reaction mixture of 4 Torr of Cl_2 and 756 Torr of O_2 flashed at 1 Hz. From these preliminary measurements, a single chemically modulated absorption band was detected at 1410-1490 cm^{-1}. This absorption exhibited the phase shift expected for a primary intermediate species, and on this basis, as well as its position,[25] the band was tentatively attributed to the ClOO radical.

The region of 1400-1520 cm^{-1} was subjected to a more intensive investigation by scanning repeatedly at a speed of 8 cm^{-1}/min. A spectrometer slit width of 6 mm was used which corresponds to a spectral width of 13 cm^{-1}. Since a time constant of 10 sec was used, a spectral slit width was covered in about ten time constants. Voltage measurements were made at 1.1-cm^{-1} intervals. These studies were made with 4 Torr of Cl_2, 189 Torr of O_2, and 567 Torr of He. These reactants were photolyzed with square-wave radiation at 2 Hz. The cumulative results of 40 such scans are shown in Figure 11a as a plot of amplitude and phase of the modulated signal vs. infrared frequency. To test reproducibility, another set of 40 scans of the 1400-1520 cm^{-1} region was recorded. The cumulative results of the second set are given in Figure 11b. The two sets of scans were then combined to obtain an improvement in signal-to-noise ratio. The combined results of 80 scans were curve-smoothed and corrected for background to obtain true absorbance. The resulting spectrum is shown in Figure 11c. Curve smoothing consisted of applying a simple three-point moving average to the raw data. Since a spectral slit width is covered by 12 data points, a three point average will not introduce distortion.

Although a chemically modulated absorption spectrum that could be attributed to the ClO radical was not detected in the exploratory spectroscopic measurements, attempts were made to observe its spectrum by means of multiple scanning over narrower spectral regions for longer periods of time. On the basis of Porter's[26] prediction of the ClO ground-state vibrational frequency (868 cm^{-1}), the observed frequencies (936, 945 cm^{-1}) of a matrix-isolated species tentatively identified as $(ClO)_2$ by Rochkind and Pimentel,[23] and the strong peak we previously observed between 930 and 980 cm^{-1}, it can be expected that the absorption band of ClO most probably lies in the region of 850-980 cm^{-1}. Therefore, this region was scanned extensively, over prolonged periods of time and under a variety of experimental conditions, in an effort to observe a modulated infrared absorption spectrum of ClO. However, these attempts proved fruitless, even under seemingly the most favorable conditions.

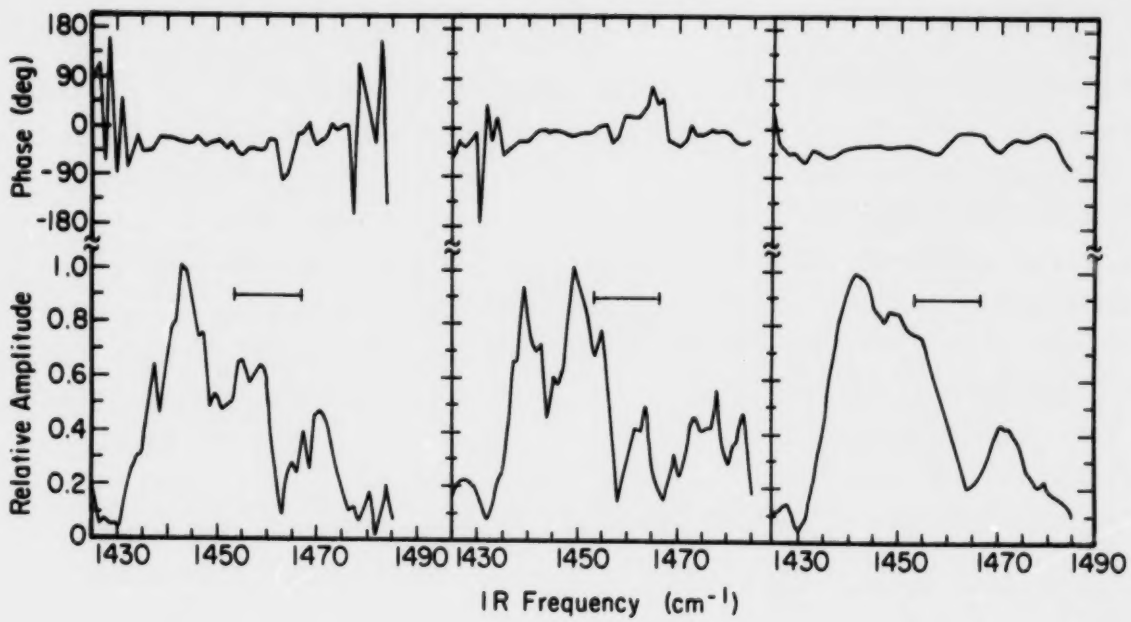

Figure 11 - ClOO infrared molecular modulation spectrum observed with 4 torr Cl_2, 189 torr O_2, 567 torr He, 2 hertz square-wave ultraviolet photolysis. a. 40 scans b. Duplicate, another set of 40 scans, c. Smoothed cumulative measurements, 80 scans (a and b). ⊢——⊣ indicates spectral slit width.

C. ULTRAVIOLET SPECTROSCOPIC MEASUREMENTS

Chlorine at 1.8 Torr in the presence of 1 atm of oxygen was photolyzed with square-wave excited lamps at 1 Hz. The rate of light absorption was estimated to be 2.4×10^{14} photons/(cm^3 sec). A modulation was observed at wavelengths between 2250 and 2900 Å, Figure 12. The measured phase angles lie in the quadrant expected for intermediates; however, the change in phase observed with wavelength indicates the presence of two or more species with overlapping absorption spectra. The small phase angle at 2300 Å represents a "fast" intermediate, that is, one whose lifetime is short compared to the flashing frequency of 1 Hz. The larger phase angle at 2800 Å indicates a much slower intermediate. The observed signal is a vector sum of the various species present.

Using literature values[14-24] for the rate of recombination of ClO and for its cross section,[21] we estimate that this species should be seen in the modulation experiment as a slow intermediate. From flash photolysis studies, ClO is known to have a banded structure from 3000 Å to the dissociation limit at 2630 Å. Porter[26] has published the locations of the vibrational band heads in this region. Experimentally it was found that reducing the total pressure to 50 Torr and flashing at 0.25 Hz increased the modulation amplitude. This allowed the spectral slit width to be reduced from 13 to 2 Å. Figure 13 shows the experimentally observed modulation amplitude together with the positions of the ClO band heads as determined by Porter. The two are in excellent agreement. Thus one of the species being observed is definitely identified as the ClO radical.

It was desired to obtain a spectrum of the fast intermediate with a minimum of interference from ClO. Since ClO is a slow intermediate, its modulation amplitude can be suppressed by increasing the flashing frequency of the photolyzing radiation. As can be seen from Figure 14, the amplitude of ClO modulation begins to fall off at a lower frequency than does the unknown, because of the difference in lifetimes. If the flashing frequency is chosen approximately equal to the lifetime of the

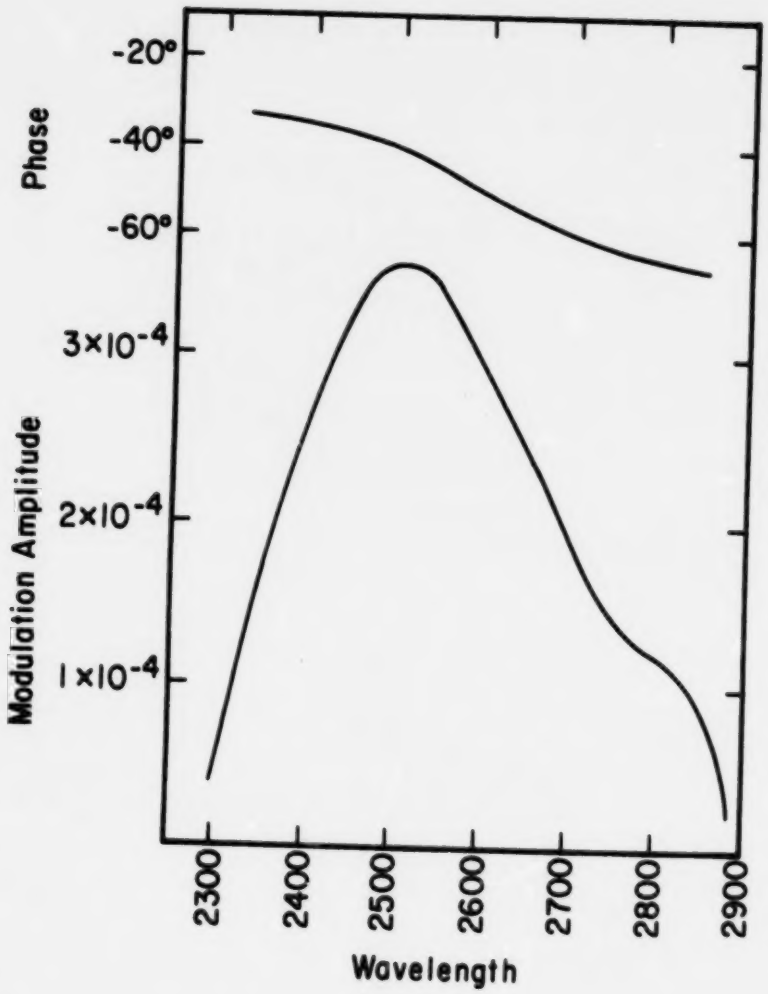

Figure 12 - ClO_x modulation spectrum in ultraviolet showing presence of two or more intermediates by virtue of change of phase shift with wavelength. 1.8 torr Cl_2, 1 atm O_2, 1 hertz square wave photolysis.

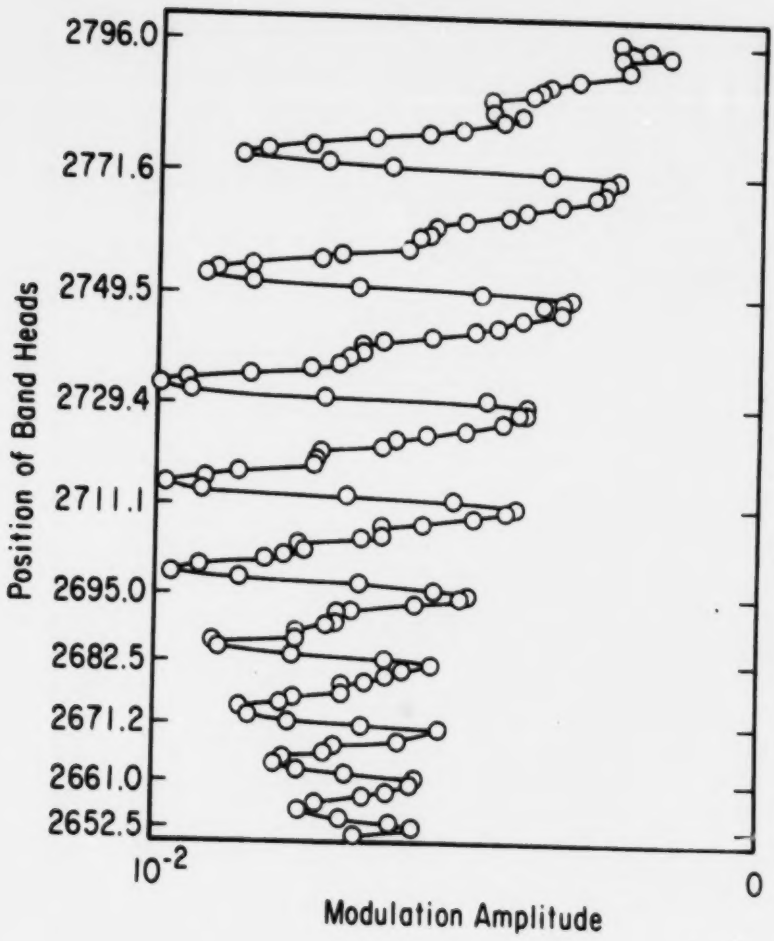

Figure 13 - Relatively high resolution molecular modulation spectrum showing vibrational structure of ClO, compared to position of ClO band heads as found by Porter (ref. 13). 4 torr Cl_2, 46 torr O_2, 1/4 hertz, spectral slit width 2A.

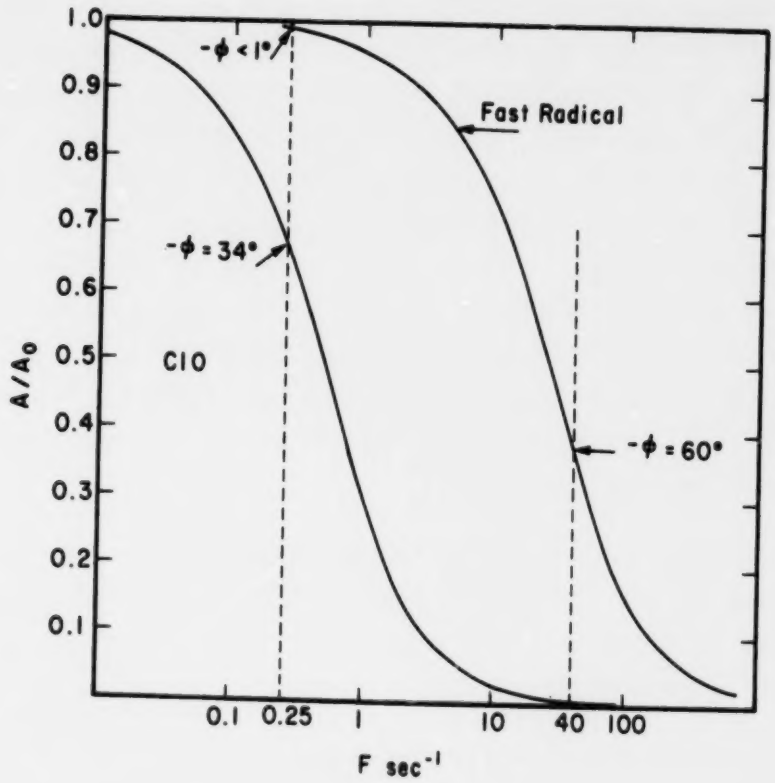

Figure 14 - Calculated relative modulation amplitude for the two ClO_x intermediates observed in this system (based on rate constants deduced later in this article, presented here to demonstrate how unwanted overlap of ClO can be reduced to zero at high frequencies and how phase of fast radical can be reduced to known zero value at low photolysis frequencies).

fast intermediate, this is much faster than the ClO lifetime. A spectrum taken at 32 Hz is given in Figure 15. The modulation spectrum extends from 2250 to 2700 Å with a maximum about 2475 Å. The phase angle is almost constant (-60 to -65°) over this range, indicating ClO modulation was effectively suppressed.

At lower frequencies the modulation is no longer simple but a vector sum of several amplitudes and phases. If this complex spectrum consists of only two species and if the phase of each is known, then the complex modulation spectrum can be factored into two components. An experiment was carried out at 0.25 Hz, Figure 16. The observed modulation shows a maximum at 2600 Å and the phase angle varies from -12° at 2300 Å to -34° at 2800 Å. From Figure 14 it can be seen that if an intermediate has a phase of -60° at 32 Hz, it would have essentially zero phase, and the plateau of -34° at 2800 Å is taken as the phase of ClO, then the observed amplitude can be decomposed into two separate spectra, one for ClO and one for the faster species, Figure 16. The spectrum of the fast radical is shown in Figure 17.

A detailed comparison of the kinetics of the fast radicals with that observed for ClOO in the infrared system identified the fast radical as ClOO. The cross sections for absorption of ultraviolet radiation by ClO and ClOO are given in Table 1.

D. MOLECULAR MODULATION MASS SPECTROMETRY

Matheson research grade Cl_2 and O_2 and high purity Ar were used directly without further purification. Gas mixtures of appropriate proportions were stored in a 5 liter glass bulb, painted black to prevent photo-reaction from room lights. Grease-free stop cocks were used throughout the system. Except for stainless steel in the flow-control valves and certain fittings, all surfaces were glass and Teflon from storage bulb to reaction cell. The pressure of the gas reaction mixture in the reaction cell was controlled by a Granville-Phillips series 9100 variable leak valve and was monitored by a Pace model CD-25 pressure

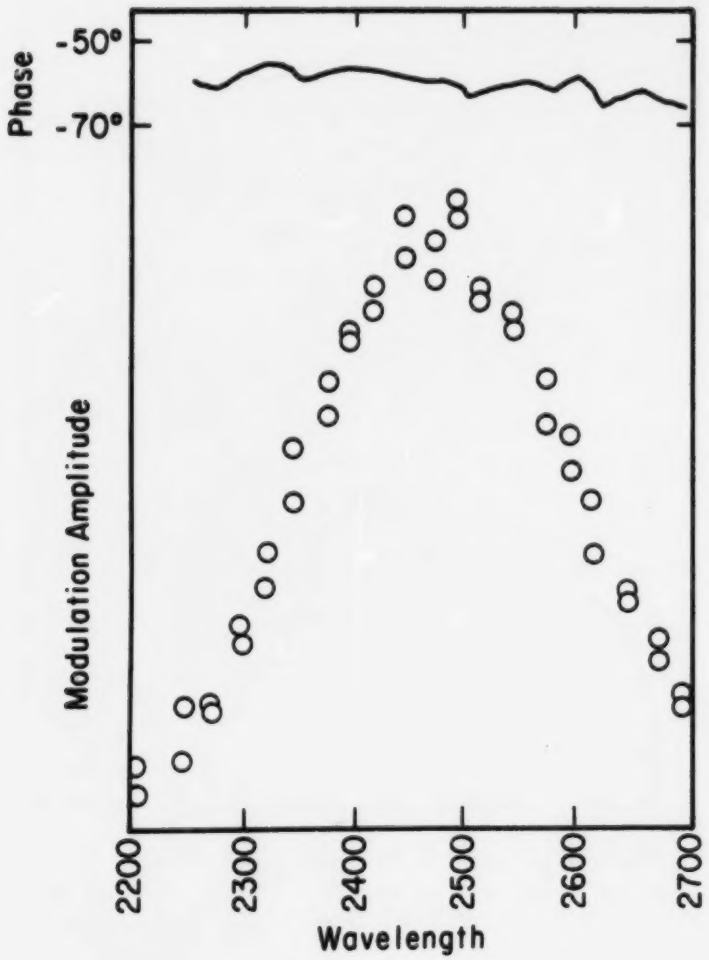

Figure 15 - Spectrum of new ClO_x species taken at high frequency, 32 hertz (compare Figure 14). The phase remains essentially constant with wavelength (contrast Figure 12).

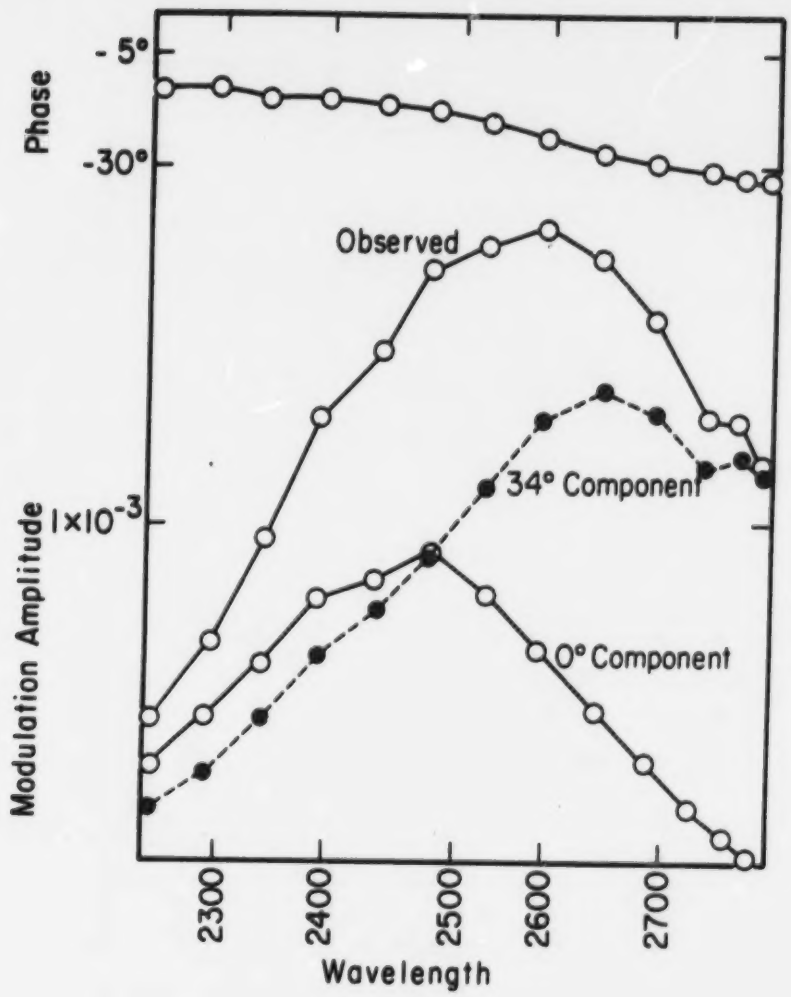

Figure 16 - Resolution of complex spectrum into two components of constant phase at low (1/4 hertz) photolysis frequency. (Compare Figure 14). The 34° component has been identified as ClO (compare Figure 13).

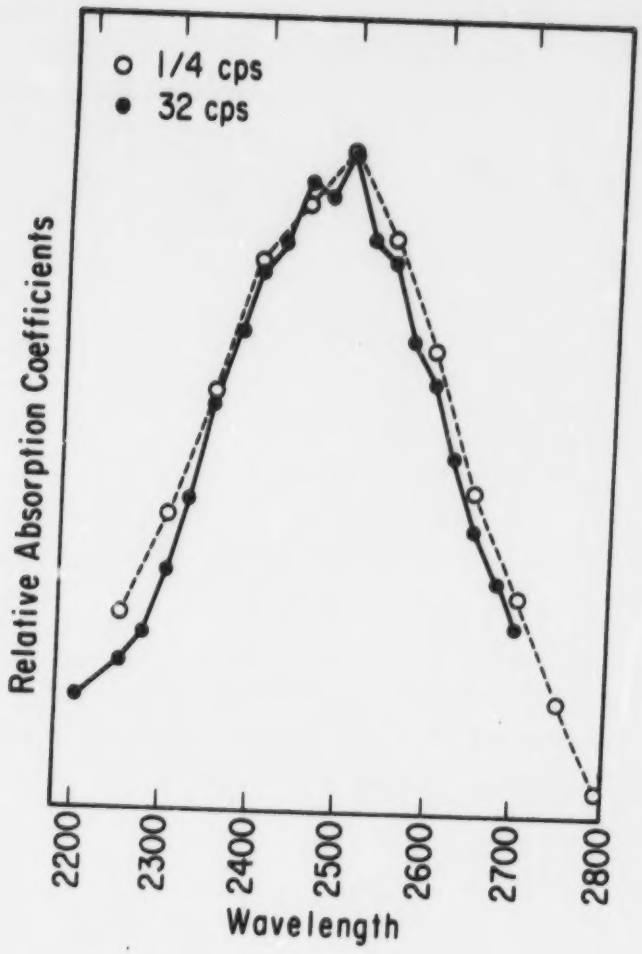

Figure 17 - Ultraviolet spectrum of ClOO radical as obtained by two different procedures.

Table 1. Absolute cross section[a] for absorption of ultraviolet radiation by the free radical ClOO and ClO in units of 10^{-18} cm^2.

λ, Å	ClOO, $\sigma_2(\lambda)$	ClO, $_1(\lambda)$[c]
2250	2.60	0.641
2300	4.91	0.846
2350	7.80	1.33
2400	10.5	1.91
2450	12.7	2.67
2500	13.3[b]	3.56
2550	12.4	4.45
2600	10.0	5.27
2650	7.28	5.68
2700	5.11	5.60
2750	3.40	4.85
2800	2.28	4.71

[a]-d ln I = σ[X]L, where concentrations are in particle/cc, L is path length in cm, and ln is logarithm to base e. [b]This work, eq 64. [c]Based on 4.83×10^{-18} cm^2 at 2577 Å by Clyne and Coxon[21].

transducer. At a cell pressure of 10 torr the typical gas flow rate was 0.008 standard cc/sec or $2x10^{17}$ molecules/sec, and the leak rate from the pin hole was $1.5x10^{16}$ molecules/sec, of which about one per cent passed through the skimmer for analysis. Five chopping speeds for the photolytic light were used: 16, 8, 4, 2 and 1 sec/cycle. For each chopping speed, from 3 to 30 measurements were taken, and each measurement involved 160 to 1600 seconds of integration time. Data were taken for both ascending and descending chopping speeds, and no significant difference was found. The photolyzing light flux was determined by NO_2 photolysis, and by a detailed comparison of absorption cross section between NO_2 and Cl_2 over the range of photolyzing light. The effective cross sections for light absorption in this range were found to be $4.65x10^{-19}$ cm^2 for NO_2 and $1.44x10^{-19}$ cm^2 for Cl_2. The photolyzing light flux was $1.35x10^{17}$ photons/cm^2 sec.

A preliminary experiment was done with a reaction mixture of Cl_2/O_2 = 1/19 at 20 torr flashed at a speed of 16 sec/cycle. Results are given in Table 2. Using the ion-counting method, we observed strong modulation signals at mass-to-charge raties (m/e) of 51 and 53. The phase shifts were identical for both signals, and the amplitude at m/e = 51 was three times that at m/e = 53, very strongly indicating it to be ^{35}ClO and ^{37}ClO. The phase of the signal at m/e = 51 did not change when the ionization energy was reduced from 40 to 20 volts, indicating that the signal was not a super-position of one mass number from two different molecules. To check against the possibility of thermal-acoustical modulations at all mass numbers, we added one-tenth per cent of Ar and searched for a modulation signal at m/e = 40. As can be seen in Table 1, the amplitudes were very small and the phases were random. A weak modulation signal was found at m/e = 67, Table 3. The small phase shift, -6.7 degrees, is kinetically correct for the $^{35}ClOO$ radical. Attempts were made to detect $^{35}Cl_2O_2$ (m/e = 102) and $^{35}Cl_2O$ (m/e = 86), but no modulation signals were obtained.

Two series of systematic experiments were performed to measure the pressure dependence and inert gas effect on the ClO disappearance rate.

Table 2. Comparison of modulated signal of ClO and unmodulated signal of Ar.

m/e	Electron Energy	(Ar)	No. Cycle	In-Phase Counter	Out-Phase Counter	Amplitude	Phase
	volts	torr	cyc	count	count	count/sec	degree
51	40	0	10	31490	9961	206	-17.5
				31099	8068	201	-14.5
				33639	9463	218	-15.7
				29815	8212	194	-15.4
						Ave 205	-15.8
53	40	0	10	11083	2958	73	-15.2
				9506	3231	64	-17.9
				10696	2571	69	-13.3
				11885	3325	77	-16.2
						Ave 71	-15.7
51	20	0	20	23213	5953	77	-14.3
				25668	7748	91	-16.8
				23775	7038	79	-15.4
				24010	8575	84	-17.9
						Ave 83	-16.1
40	40	0.02	10	-272	-301	1.8	+131.7
				-163	421	2.8	-111.2
				+75	+198	1.2	-69.5
				+336	-219	1.3	+33.0
				-139	+284	2.0	-116.1
						Ave 1.8	-26.5

$[Cl_2]$ = 1 torr, $[O_2]$ = 19 torr, chopping period = 16 Hz.

Table 3. Comparison of modulated signal of ClOO and ClO.

m/e	Electron Energy	(Ar)	No. Cycle	In-Phase Signal	Out-Phase Signal	Ampli-tude		Phase
	volts	torr	cyc	count	count	count/sec		degree
67	40	0.04	800	14206	1569		18	-6.3
				16983	2442		21	-8.2
				24733	2195		24	-5.1
				11825	1496		15	-7.2
						Ave	19	-6.7
51	40	0.04	200	37295	48872		307	-52.7
				36142	49102		304	-53.5
				36998	47767		295	-52.2
				35872	49413		306	-54.3
						Ave	303	-53.2

$[Cl_2]$ = 2 torr, $[O_2]$ = 38 torr, chopping period = 1 Hz.

In one series the ratio Cl_2/O_2 was maintained at 1/19, the total pressure was varied from 40, 20 10 to 5 torr, and the chopping speeds were 16, 8, 4, 2 and 1 sec/cycle. In the second series the reactants were held constant (Cl_2 = 0.75 torr, O_2 = 6.75 torr), and Ar was varied as 0, 5, 17.5, and 42.5 torr to give total pressure of 7.5, 12.5, 25, and 50 torr. The phases for both of these series are given in Table 4 and some of the data are plotted in Figures 18 and 19.

Table 4. Observed phases as a function of chopping frequency and concentrations.

Pressure, torr				Flashing period, sec/cycle				
Total	Cl_2	O_2	Ar	16	8	4	2	1
40	2	38	0	-10.8	-15.5	-23.4	-36.7	-53.1
20	1	19	0	-15.9	-24.3	-36.3	-60.9	-76.3
10	0.5	9.5	0	-21.6	-34.5	-53.8	-77.1	-96.4
5	0.25	4.75	0	-40.7	-63.1	-74.5	-91.3	-
7.5	0.75	6.75	0	-20.5	-30.1	-45.5	-66.0	-80.5
12.5	0.75	6.75	5	-17.0	-23.5	-39.8	-61.3	-78.8
25.0	0.75	6.75	17.5	-13.7	-17.8	-33.1	-54.8	-75.4
50.0	0.75	6.75	42.5	- 6.4	-11.7	-26.5	-46.1	-67.0

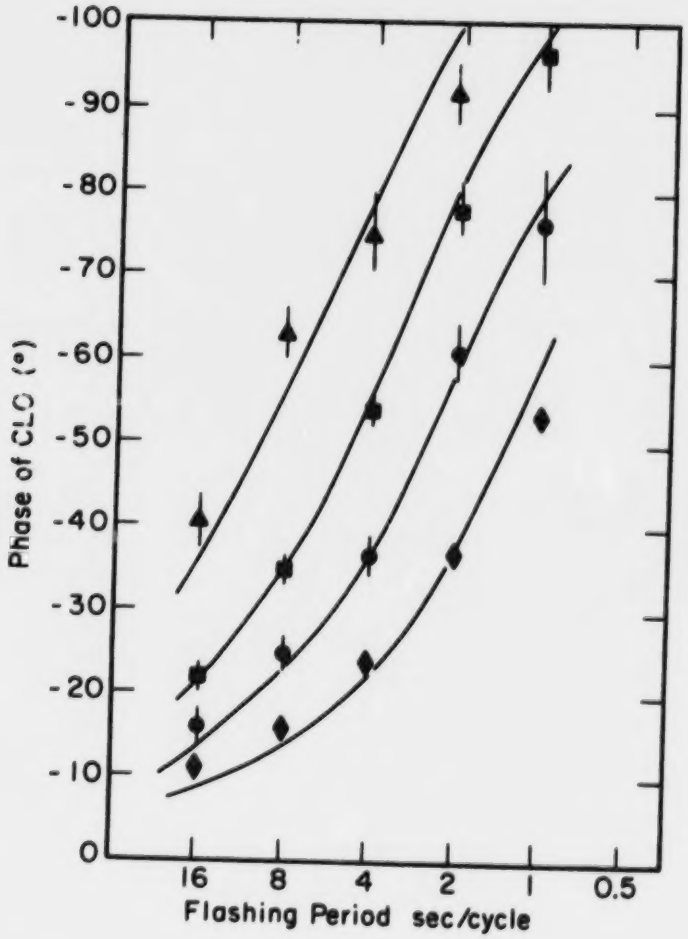

Figure 18 - Observed points and calculated curves for the phase shift of ClO in a mixture of 5% Cl_2 and 95% O_2. Total pressure in torr: ▲, 40; ■, 20; ●, 10; ▲, 5.

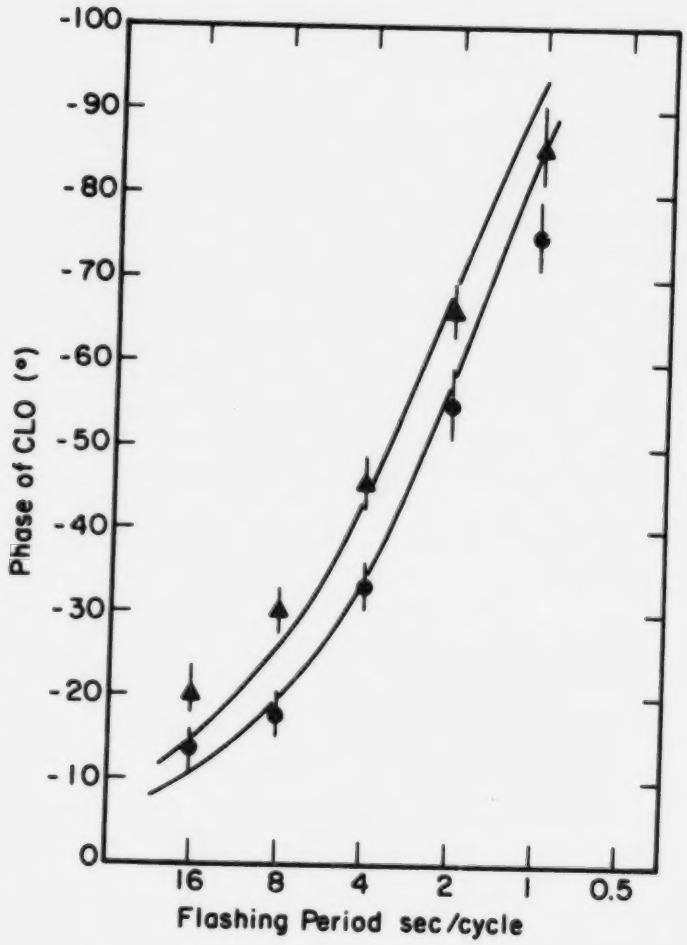

Figure 19 - Observed points and calculated curves for the phase shift of ClO in a mixture of Cl_2 = 0.75 torr, O_2 = 6.75 torr, and Ar in torr: 0, 17.5; Δ, zero.

SECTION VII

SPECTRA AND KINETICS OF THE HYDROPEROXYL FREE RADICAL

A. INTRODUCTION

The occurence of HOO as an intermediate has been postulated in kinetic studies of the hydrogen-oxygen reactions,[27-33] in photochemical studies of ozone in the presence of water[24-37] or in the presence of hydrogen peroxide,[38] and in the photolysis of hydrogen peroxide.[39] In a study of the flash photolysis of hydrogen peroxide with direct observation of the hydroxyl radical, Greiner[40] showed that hydroxyl is formed directly by photolysis

$$H_2O_2 + h\nu \rightarrow 2HO$$

and that it decays by a process first order in HO and first order in H_2O_2, presumably

$$HO + H_2O_2 \rightarrow H_2O + HOO$$

Greiner searched for an absorption by HOO in the region 2500 - 10,000 Å but found nothing. The overall kinetics of the photolysis of hydrogen peroxide indicates the following reaction as the radical terminating step

$$HOO + HOO \rightarrow H_2O_2 + O_2$$

Direct observation of HO_2 was first accomplished by Foner and Hudson[41] who succeeded in producing hydroperoxyl radicals by the reaction

$$H + O_2 + M \rightarrow HO_2 + M$$

and detecting them by mass spectrometry. This radical has also been observed mass spectrometrically by Robertson[42] who added O_2 to a stream of H atoms, Ingold and Bryce[43] who reacted O_2 with H atoms and with

methyl radicals, and Fabian and Bryce[44] who studied the reaction of methane with oxygen molecules. Foner and Hudson[41] have reported observing the mass spectrum of HO_2 formed in six different ways: the reactions of H atoms with O_2 and H_2O_2, of O atoms with H_2O_2, of OH radicals with H_2O_2, the photolysis of H_2O_2, and a low-power electrical discharge of H_2O_2.

Spectroscopic detection of HO_2 has been achieved by Milligan and Jacox[45] using the matrix isolation technique. They photolyzed an HI-O_2 mixture in an argon matrix at 4°K and obtained infrared absorption peaks in the regions 1040 - 1101 cm^{-1}, 1380 - 1390 cm^{-1}, and at 3402 and 3414 cm^{-1}. These absorptions were attributed to the O-O stretching, HOO bending, and H-O stretching vibrations, respectively. The spectrum has been confirmed by Ogilvie[46] in an argon-neon matrix at 4°K, but his low frequency assignments are reversed.

The transient ultraviolet absorption spectrum of HO_2 has been observed following the pulsed electron irradiation of oxygenated aqueous solutions by Czapski and Dorfman.[47] The spectrum of the radical in solution begins at approximately 3000 Å and has a maximum at 2300 Å with a molar extinction coefficient α = 1150 M^{-1} cm^{-1}. Subsequent experiments in pulse radiolysis and flash photolysis of aqueous solutions have confirmed the u.v. spectra.[47]

Troe[48] observed the ultraviolet spectrum of gaseous HOO between 2100 and 2800Å at 1100°K in the thermal decomposition of hydrogen peroxide in a shock tube. Hochanadel and coworkers[49] have observed the ultraviolet spectrum of HOO and the rate constant for the reaction

$$HOO + HOO \rightarrow H_2O_2 + O_2$$

Also, Foner and Hudson have obtained a value for this rate constant.

B. THE INFRARED SPECTRUM AND KINETIC RESULTS

Molecular modulation absorption spectra were recorded while an ozone-hydrogen peroxide mixture in helium was being illuminated by the

photolytic lamp flashing at 1.4 Hz. The ozone concentration was about 5×10^{14} molecules/cc; the peroxide concentration was about 5×10^{15} molecules/cc. The two reactants were diluted by helium at atmospheric pressure. The spectrometer slits set to 6 mm correspond to an average resolution of 12 cm^{-1}. Figure 20 shows the modulated absorption of ozone from 1050 to 1075 cm^{-1}; the phase shift of the ozone modulation is +85°, which is in the quadrant proper to a reactant destroyed by both the photolytic light and radical attack. Absorption by a second species displays a maximum at 1127 cm^{-1}. The phase shift of the second species is -35° which is proper for a radical intermediate. The breadth of the region with radical phase shift (1080 to 1140 cm^{-1}) indicates that the absorption by the second species is quite broad and may well extend below 1080 cm^{-1}, but the ozone absorption is so intense that it obscures all else.

The photolysis of ozone and hydrogen peroxide at 1.4 Hz under the same chemical conditions as above was studied in the infrared region 1340 to 1500 cm^{-1} (Figure 21). The resolution in this region with the slits opened to six mm is 12 cm^{-1}. Another spectrum of this region, obtained under a resolution of 8 cm^{-1}, is shown in Figure 22. Both spectra show a strong absorption with a radical phase shift between 1350 and 1440 cm^{-1}. An absorbance minimum occurs at 1390 cm^{-1}. The sharp peaks at 1408 and 1425 cm^{-1} in Figure 21 and at 1368, 1378, and 1425 cm^{-1} in Figure 22 are narrower than the resolution of the spectrometer and cannot be regarded as spectral features. The spectrum in this region then consists of a pair of peaks centered at 1390 cm^{-1} and separated by about 42 cm^{-1}.

The last region in the infrared which shows modulated absorption is between 3300 and 3605 cm^{-1}. This region was studied under the same chemical conditions as the previous two at a flashing frequency of 1.4 Hz. The resolution in this region varied from 18 to 25 cm^{-1}, at 3300 cm^{-1} to at 3600 cm^{-1}. The modulated absorption spectrum shown in Figure 23 is the result of sixteen scans and a three point curve smooth.

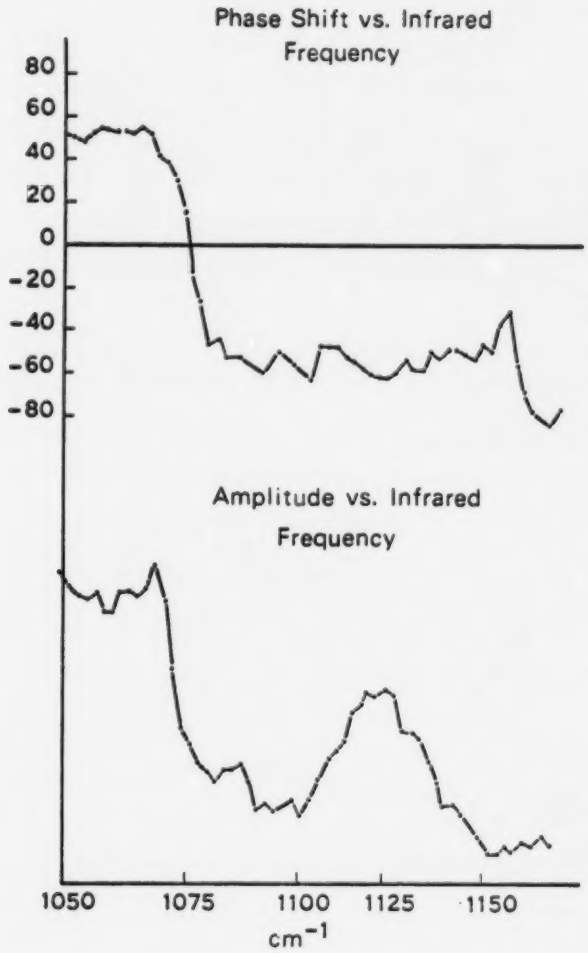

Figure 20 - The modulated infrared absorption spectrum (1050 to 1150 cm^{-1}) obtained during the photolysis of ozone in the presence of hydrogen peroxide.

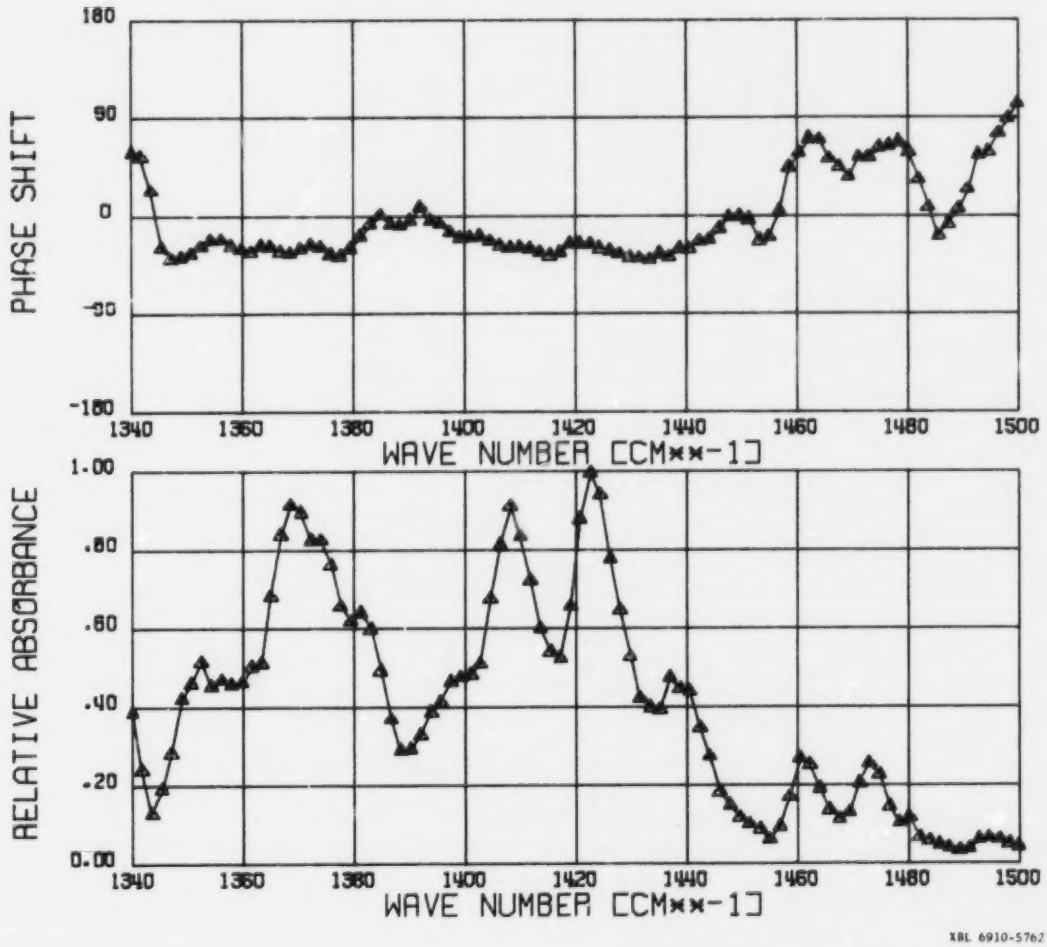

Figure 21 - The modulated absorption spectrum obtained during the photolysis of ozone in the presence of hydrogen peroxide at 1.4 Hz. Six repetitive scans at 12 cm^{-1} resolution and a three-point curve smooth.

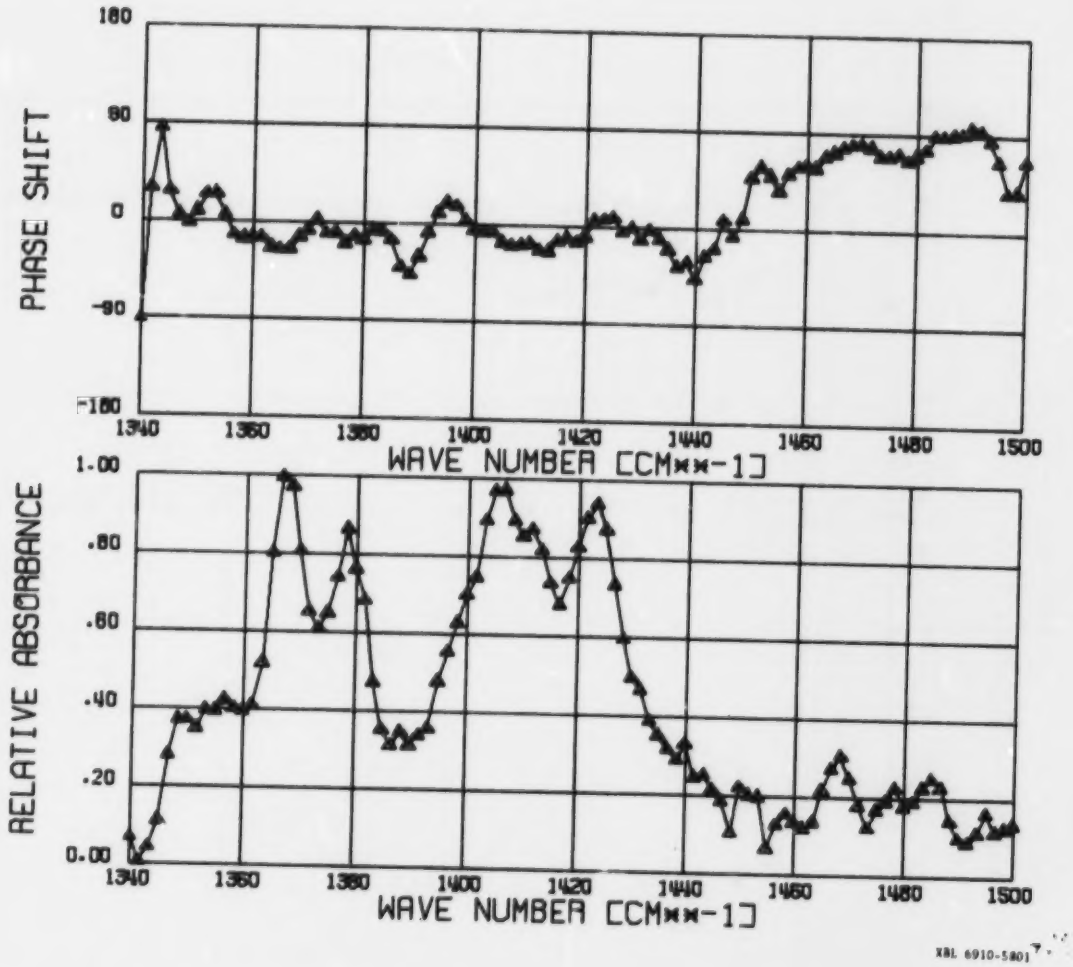

Figure 22 - The modulated absorption spectrum obtained during the photolysis of ozone in the presence of hydrogen peroxide at 1.4 Hz. Eleven repetitive scans at 8 cm^{-1} resolution and a three-point curve smooth.

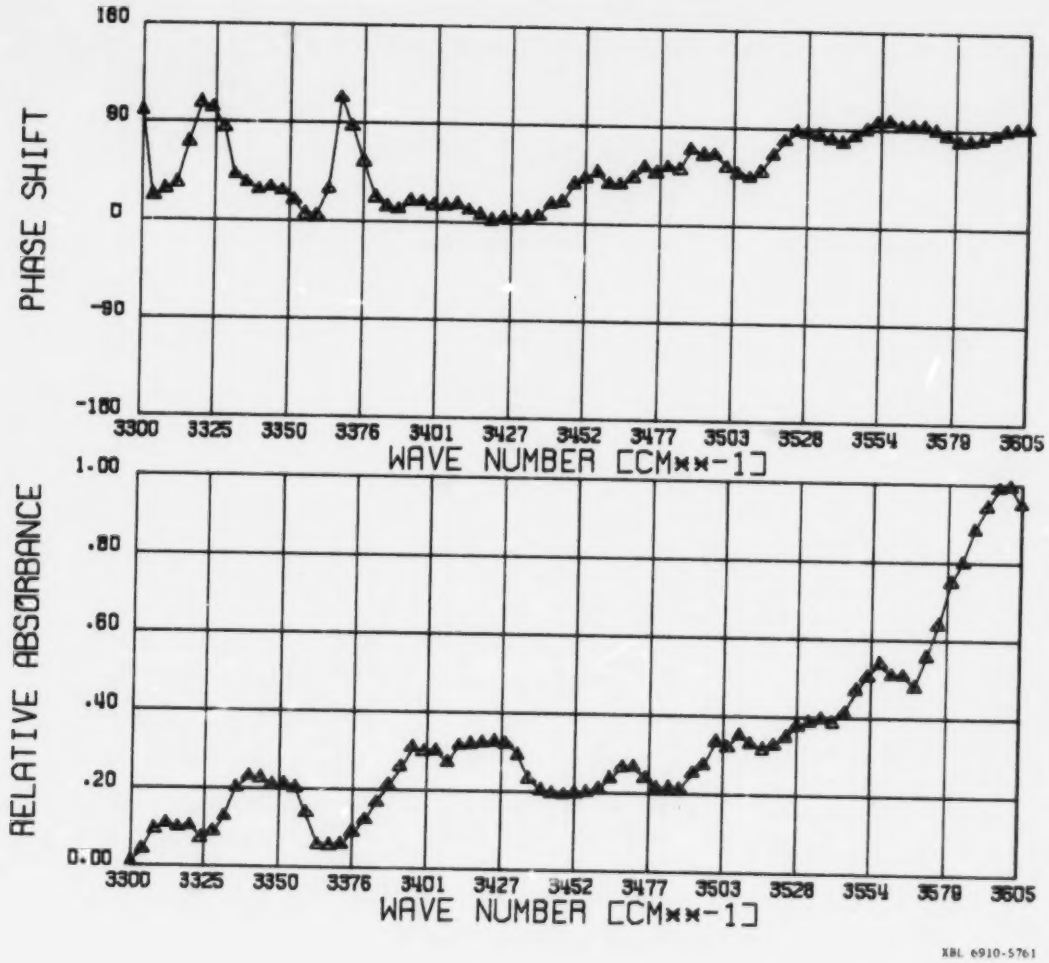

Figure 23 - The modulated absorption spectrum obtained during the photolysis of ozone in the presence of hydrogen peroxide at 1.4 Hz. The spectrum is the average of sixteen scans and a three-point curve smooth.

The absorption maximum at 3600 cm^{-1} is very similar to the hydrogen peroxide peak and has a +90° phase shift due primarily to hydrogen peroxide. At lower infrared frequencies new absorption peaks are evident which cannot be assigned to either hydrogen peroxide or water because the new absorption is strongest where both water and peroxide absorption is weak, i.e., between 3350 and 3450 cm^{-1}. Furthermore, the phase shift of the new absorption is displaced toward the radical quadrant, but the phase shift never reaches a constant value typical of single species absorption so there must still be some peroxide component in the signal. In addition to the main peak which extends from 3380 to 3440 cm^{-1}, there are several smaller peaks at 3550, 3505, 3470, 3345, and 3312 cm^{-1}. These peaks are not present in the spectrum of water or hydrogen peroxide. The pattern of peaks does not fit the position of Q and P branch lines of the OH radical[45] which is known to be present in this chemical system. Later it will be shown that these peaks are consistent with the best current estimates of the structure of HOO.

During the photolysis of hydrogen peroxide the dependence of the modulated absorption peaks at 1075, 1120, 1373, and 1420 cm^{-1} on flashing frequency was studied. In these experiments the infrared spectrometer was set at a fixed I.R. frequency and the modulation signal was recorded by the computer every 10 sec for a period of ten to thirty min. The hydrogen peroxide concentration was 5×10^{15} molecules/cm^3. The helium carrier gas at a pressure of one atmosphere flowed through the cell at 8.4 l/min. Room temperature during these runs was 22°C. Flashing frequency was varied from 1/4 Hz to 4 Hz.

The observed phase shifts, each the result of from ten to thirty min. of averaging, are plotted in Figure 24. The average phase shift at each flashing frequency is indicated in Figure 24 by an arrow. The solid curve in the figure is the calculated curve for a second-order radical. The position of the calculated curve on the time axis gives the quantity $(PQ)^{1/2}$; it is 5.55 sec^{-1}.

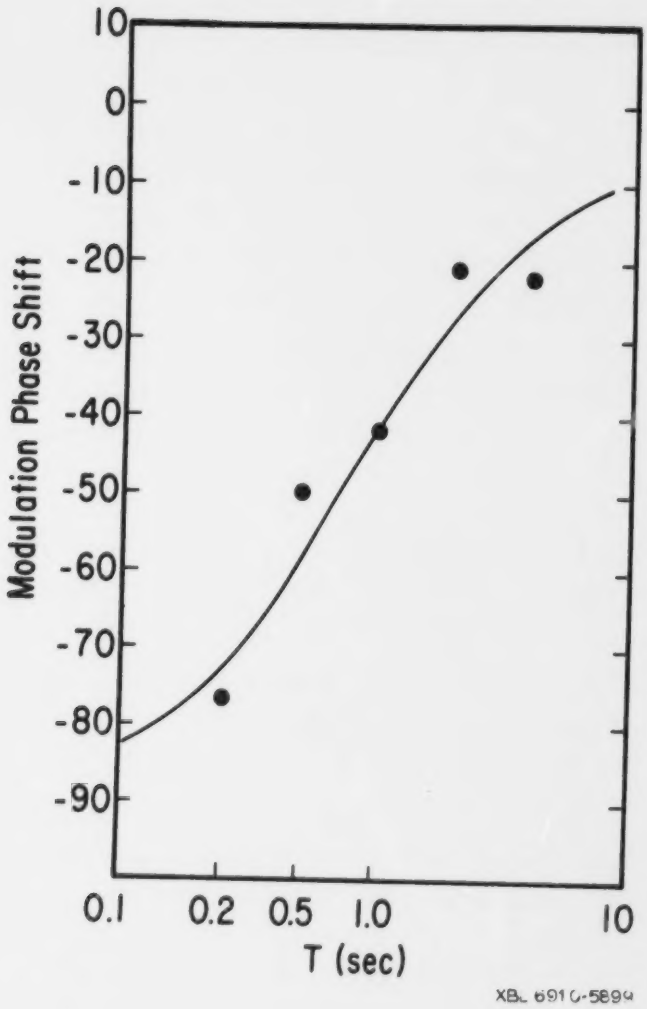

Figure 24 - Phase shift of the infrared absorption peaks as a function of flashing period. x = 1075 cm^{-1}; ○ = 1120 cm^{-1}; □ = 1373 cm^{-1}; Δ = 1420 cm^{-1}; ● = Average of all points.

C. THE ULTRAVIOLET SPECTRUM

Two series of experiments were carried out in obtaining the ultraviolet spectrum of HOO between 1950 and 2500 Å. In one series H_2O_2 in one atmosphere of He was photolyzed at 2537 Å. The mechanism is presumably reactions (1), (2), and (3). In the other system, chlorine was photolyzed between 3200 and 3800 Å in the presence of H_2O_2. The expected elementary reactions are

$$Cl_2 + h\nu \rightarrow 2Cl$$

$$Cl + H_2O_2 \rightarrow HCl + HOO$$

$$HOO + HOO \rightarrow H_2O_2 + O_2$$

In a preliminary experiment, a modulation absorption spectrum was obtained from 2450 to 2000 Å during the photolysis of H_2O_2 at 1×10^{16} molecules/cc, at 1 Hz photolysis frequency, in an atmosphere of helium flowing at 8.4 l/min. The modulation absorption was measured at 50 Å intervals with a spectral resolution of 13.3 Å. The spectrum showed an absorption band with a peak at 2100 Å, with phase shift between -15.8° and -24.0° (which is in the radical quadrant), and a variation of phase shift with wave length that suggests the presence of two modulated species. The same spectral region was examined at 1/4 Hz, and the results are shown in Figure 25. At this frequency the phase shift of the modulation displays a strong dependence on wave length, clearly indicating the presence of two species one of which is relatively more important at 1/4 Hz than at 1 Hz.

Since the phase shift at 1/4 Hz is in a reactant quadrant and since reactant amplitudes show a stronger dependence on flashing frequency than do radical amplitudes, the species gaining importance at 1/4 Hz must be the reactant hydrogen peroxide. The shape of the hydrogen peroxide absorption spectrum is well-known[50,51] and agrees closely with the spectrum obtained in our laboratory. It is evident that hydrogen peroxide could be contributing to the modulated spectrum.

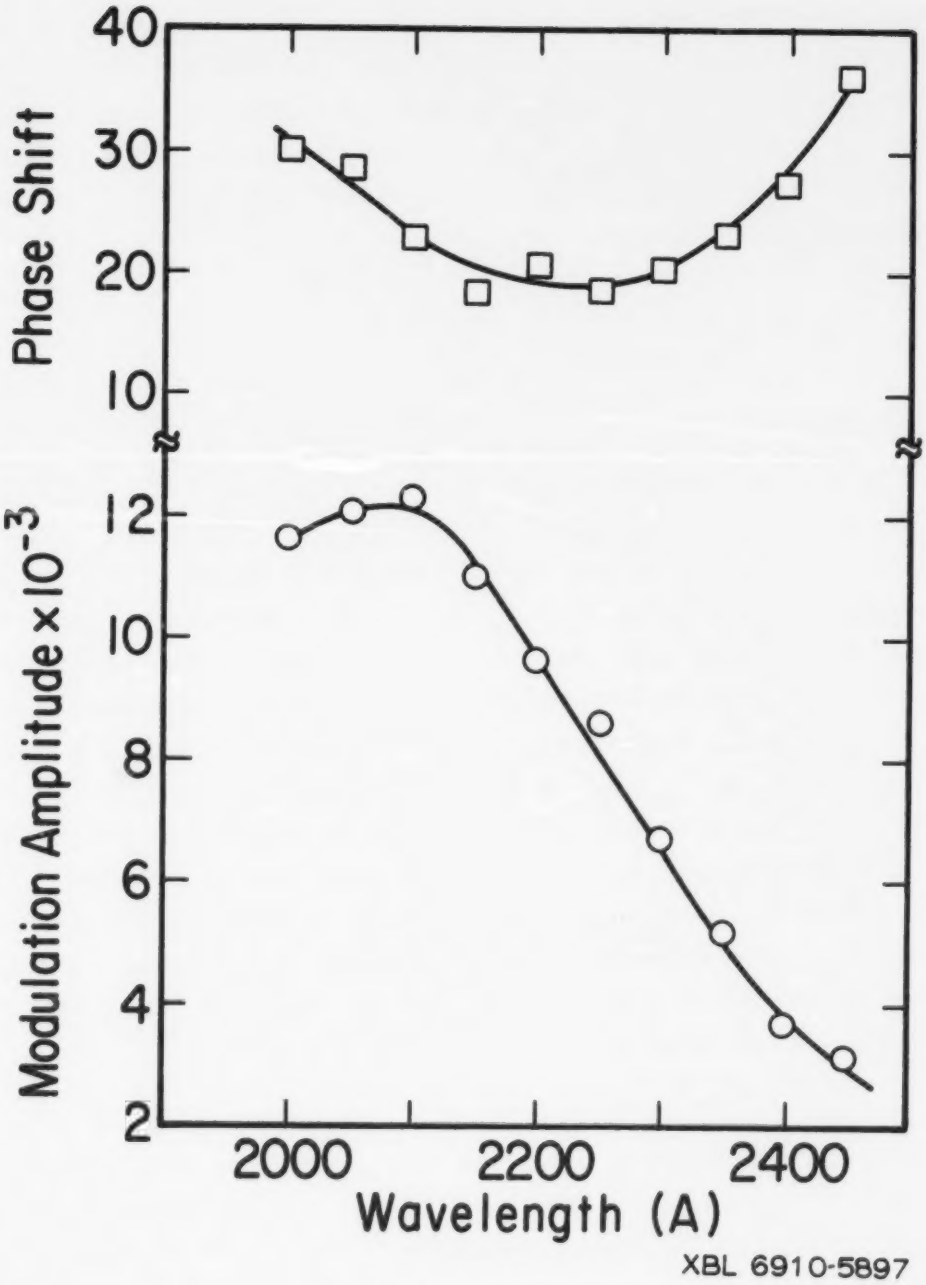

Figure 25 - The modulated ultraviolet absorption spectrum obtained during the photolysis of hydrogen peroxide by one lamp at 1/4 Hz.

The response of the modulated absorption at 2200 Å to variations in flashing frequency was studied from 1/4 to 32 Hz. The conditions of the experiment were set as closely as possible to the conditions under which the spectrum (Figure 25) was obtained; the hydrogen peroxide concentration was 1.13×10^{16} molecules/cm^3. The phase shift is plotted against log T where T is flashing period in Figure 26; the theoretical second-order radical curve is included in the figure for comparison with the observed results. At low frequencies the observed phase shift is too positive for a pure radical signal. Apparently a reactant is becoming progressively more important as the flash period increases, agreeing with the previous results.

Two modulation spectra that overlap in wave length can be resolved if the kinetic behavior (phase shift) of the two species is substantially different. The mechanism is rewritten in the following way

$$H_2O_2 + h\nu \rightarrow 2HO$$

$$2HO + 2H_2O_2 \rightarrow 2H_2O + 2HOO \qquad \text{(fast)}$$

$$2HOO \rightarrow H_2O_2 + O_2$$

Three molecules of H_2O_2 disappear with absorption of one photon, and two molecules of HOO are formed. Two molecules of HOO disappear according to the third reaction, and one molecule of H_2O_2 is reformed. From this mechanism the differential equations are

$$\frac{d[H_2O_2]}{dt} = -3\sigma_2[H_2O_2]\ I + k_3[HOO]^2$$

$$\frac{d[HOO]}{dt} = 2\sigma_2[H_2O_2]\ I - 2k_3[HOO]^2$$

The steady-state relations are

$$[HOO]_{ss} = (\sigma_2[H_2O_2]I/k_3)^{\frac{1}{2}}$$

$$\tau_{ss} = (4k_3\sigma_2[H_2O_2]I)^{-\frac{1}{2}}$$

The values of light intensity I, average peroxide concentration, and peroxide absorption cross section σ_2 are known. For square wave photolysis of period T, the concentration profiles of both H_2O_2 and HOO can be calculated uniquely for a given value of the ratio of period T to steady-state half-life τ_{ss}

$$\rho = T/\tau_{ss}$$

These concentration profiles were computed for a wide range of values of ρ, 0.05 to 333; and fourier analyses of the concentration profiles gave the fundamental amplitude and phase shift. At flashing frequencies of 8 Hz or greater, the reactant amplitude is so small that it may be neglected entirely; and the resulting plot of phase shift against flashing frequency (Figure 26) gives the value of ρ. With our tables of phase and amplitude as a function of ρ, the observed signal can be decomposed into radical amplitude and reactant amplitude from the observed net phase shift. This procedure is tested for the 1/4 Hz data of Figure 25, and the results are given in Figure 27. The observed resolution of amplitude from the experimental data agrees very well with the theoretical curve, which justifies the application of this treatment of the data. With the availability of this method of resolving the overlapping spectra, an extensive set of data were taken over a wide range of wavelength and photolysis periods.

In another set of experiments, modulation spectra of the entire 2450 to 2000 Å region were obtained at flashing frequencies from 1/4 to 16 Hz. The spectra were acquired at 50 Å intervals with a resolution of 13.3 Å. The hydrogen peroxide was again carried into the reaction cell by a stream of helium flowing at 8.4 l/min. Two photolysis lamps were used. Because of the greater light intensity, the hydrogen peroxide concentration was lower than in the previous experiment. The concentration of peroxide in the two-lamp experiment was 8.5×10^{15} molecules/cm^3. The observed spectra acquired at the various flashing frequencies in this experiment are shown in Figures 28 and 29. Each spectrum has its most negative phase shift between 2150 and 2250 Å usually at 2200 Å. The phase shift at 2200 Å is plotted against log T and the model curve is fitted to the high frequency data, i.e., 2, 4, and 8 Hz. The spectrum at 16 Hz is not used here because it is quite noisy. The 1/4 Hz spectrum

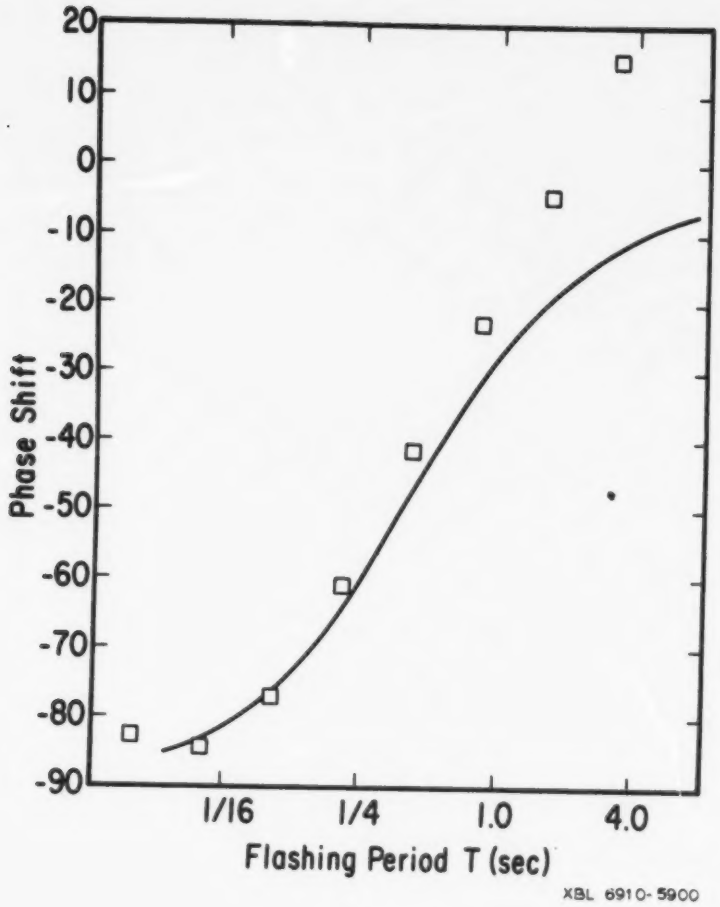

Figure 26 - The dependence of the phase shift of the modulation at 2200 Å on flashing period. The curve is the calculated curve for a primary second-order radical. Only one photolysis lamp was used.

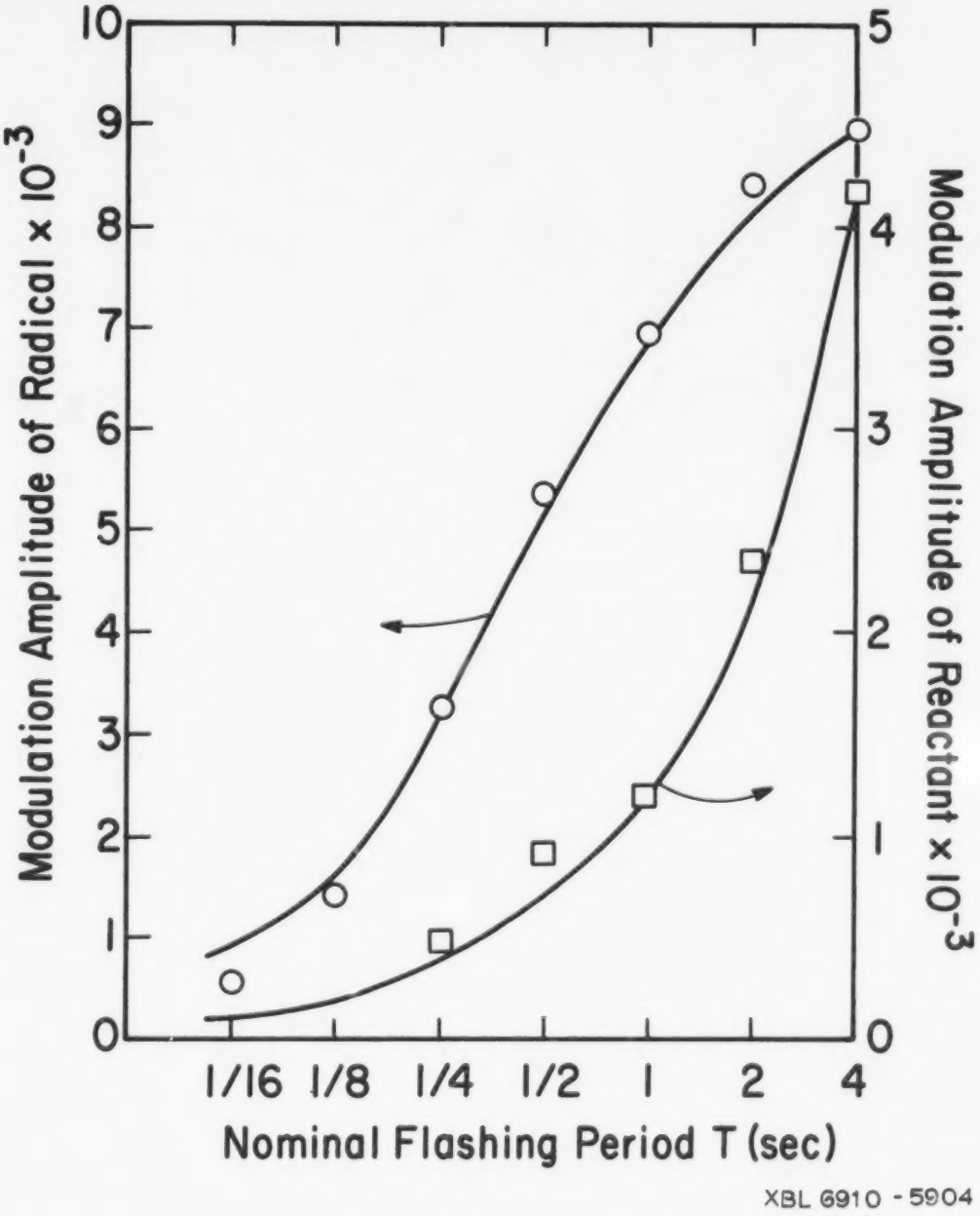

Figure 27 - Comparison of radical and reactant amplitudes extracted from the data with the amplitudes predicted by the mechanism. ○ = Radical amplitude; □ = Reactant amplitude. Solid curves are the amplitudes predicted by the mechanism.

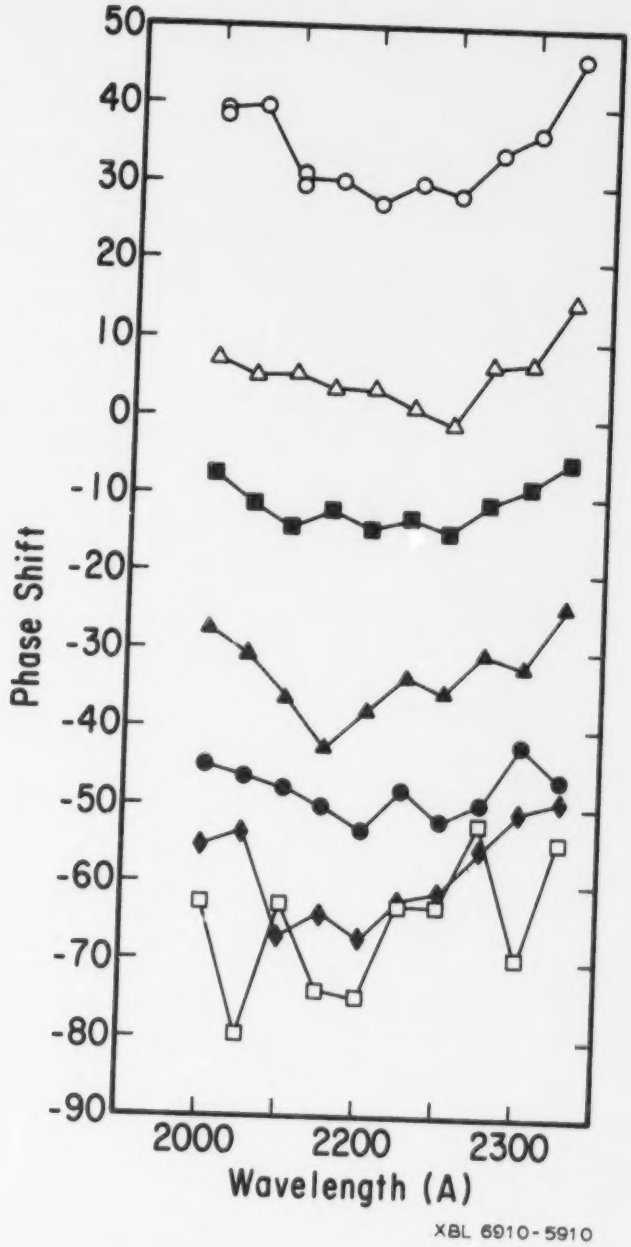

Figure 28 - The modulated absorption phase shifts from 2450 to 2000 Å obtained during the photolysis of hydrogen peroxide by two lamps. ○ = 1/4 Hz; △ = 1/2 Hz; ■ = 1 Hz; ▲ = 2 Hz; ● = 4 Hz; ◆ = 8 Hz; □ = 16 Hz.

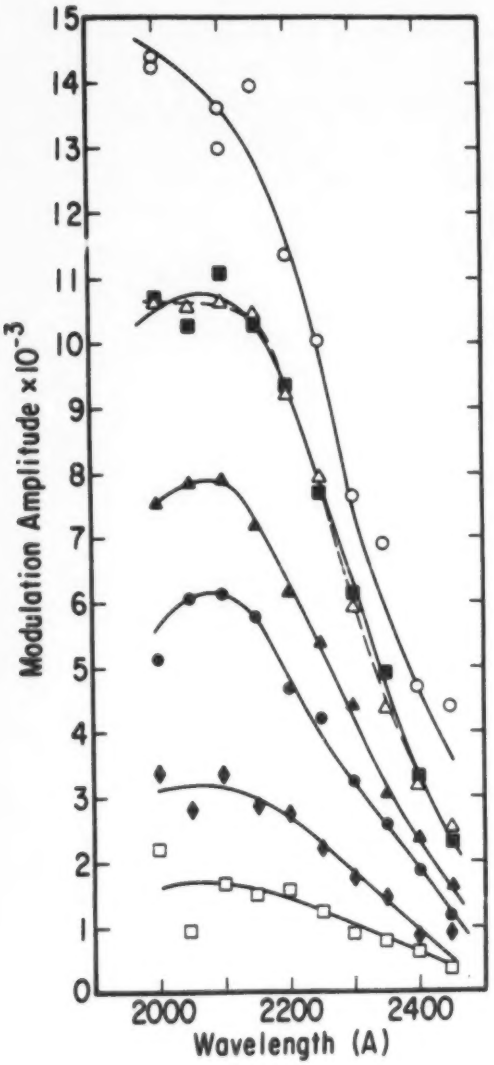

Figure 29 - The modulated absorption amplitudes from 2450 to 2000 Å obtained during the photolysis of hydrogen peroxide by two lamps. ○ = 1/4 Hz; Δ = 1/2 Hz; ■ = 1 Hz; ▲ = 2 Hz; ● = 4 Hz; ♦ = 8 Hz; □ = 16 Hz.

is decomposed into -8.2° and 93.7° components. The 93.7° component is fit by the method of least squares to the known hydrogen peroxide spectrum to obtain the amplitude of the peroxide modulation at 1/4 Hz. The phase shift and amplitude behavior of the reactant as a function of flashing frequency is known from the model, so the reactant contribution at each flashing frequency can be calculated and subtracted from the experimental data to get the modulation signal of the radical at each flashing frequency and measured wave length.

The average phase shift of the radical over the 2000-2500Å region is plotted against log T (Figure 30).

A curve results that fits the second-order radical function within the experimental error. The position of the curve gives a value of $(PQ)^{1/2}$ of 14.5 sec^{-1}.

D. THE DISPROPORTIONATION RATE CONSTANT

The differential equation for HOO radical formation and second-order decay may be written (compare Eq. 16)

$$\frac{dX}{dt} = P - QX^2$$

The correlation of phase shift with photolysis period (Figures 24, 26, 30) gives the product PQ. The difference in H_2O_2 decomposition in the light and in the dark gives P. The rate constant k_3 is thus given by

$$k_3 = \frac{Q}{2} = \frac{(PQ)}{2P}$$

With respect to this rate constant, the results from the infrared (Figure 24) and ultraviolet (Figures 26 and 30) studies are combined. The value of the rate constant is

$$k_3 = (3.6 \pm 0.5) \times 10^{-12} \text{ cc/particle-sec.}$$

where k_3 is defined by

$$-\frac{d[HOO]}{dt} = 2k_3[HOO]^2$$

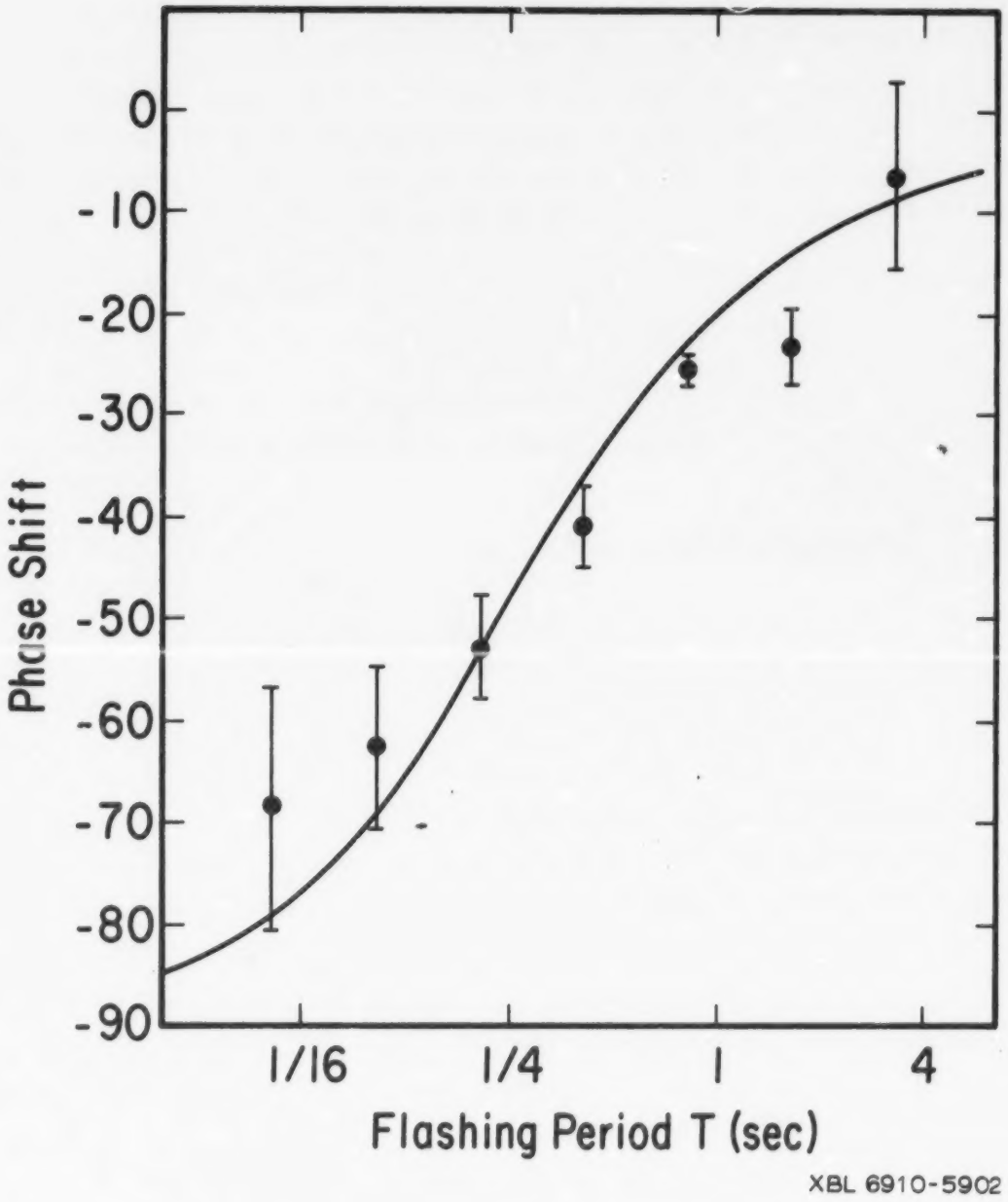

Figure 30 - The phase shift of the radical vs the flashing period. The curve is the calculated curve for a primary second-order radical.

E. ABSORPTION COEFFICIENTS OF THE HYDROPEROXYL RADICAL

The absorption coefficient σ is defined by the equation $-\Delta I/I = \sigma \Delta n l$ for small changes in the transmitted light intensity through an absorbing medium of length l caused by small changes in the concentration of the absorbers Δn. In our spectroscopic systems, the optical path length is known and the modulated absorbance $\Delta I/I$ is measured. In the limit of very long photolysis periods T the radical amplitude is given by

$$\Delta n = [HOO]_{ss} = (P/Q)^{1/2}$$

The observed quantities are P and PQ. Thus

$$\Delta n = P/(PQ)^{1/2}$$

The absorbance $\Delta I/I$ is measured at finite flashing frequencies and must be corrected to the low frequency limit. The observed phase shift and the model second-order radical curves specify the ratio of measured absorbance at each flashing frequency to the absorbance at the low frequency limit. The experiments in the ultraviolet cell provide a considerable body of data from which to calculate the cross-section for absorption. From the two-lamp experiment the spectra obtained at 1/4, 1, 2, and 4 Hz were used to determine the absorption coefficient. (The amplitude of the spectrum at 1/2 Hz is not used because it is abnormally small). Both the spectra at 1/4 and 1 Hz obtained from one-lamp experiments were used for another determination of the absorption coefficient. At the absorption peak of the hydroperoxyl radical its absorption coefficient is to the base e: 4.5×10^{-18} cm^2/molecule; to the base ten: 2.0×10^{-18} cm^2/molecule. The absorption coefficient of this radical at its peak has been found in aqueous solution[40] to be (base 10): 1.9×10^{-18} cm^2/molecule. The absorption cross section as a function of wave length between 1950 and 2450 Å is given by Figure 31.

The infrared absorption of HO_2 is strongest at 1420 cm^{-1} where $\Delta I/I$ is observed to be 1.56×10^{-4} under conditions which give the radical a

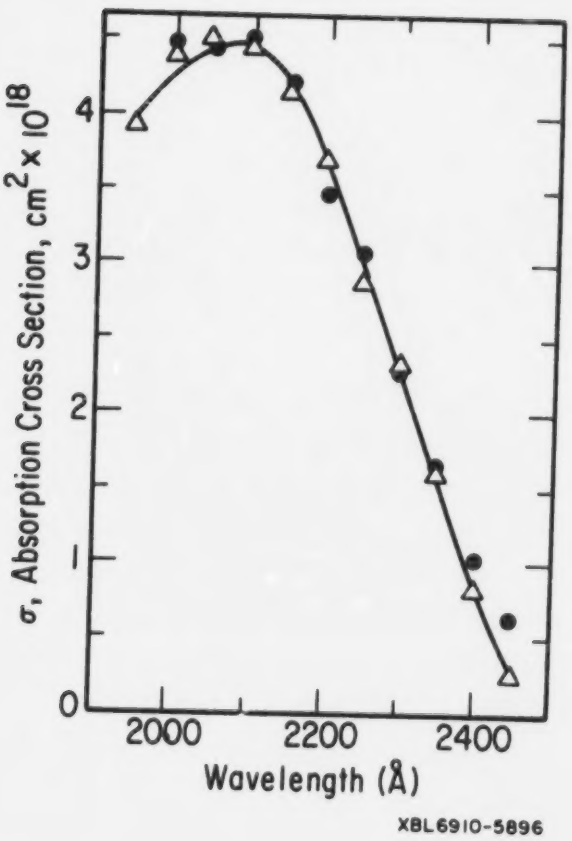

Figure 31 - The ultraviolet spectrum of the hydroperoxyl radical, $-dI = \sigma I L dN$. ● = Average of all the ultraviolet spectra obtained from the photolysis of hydrogen peroxide at 2537 Å; Δ = The spectrum from the photolysis of chlorine in the presence of hydrogen peroxide at 3600 Å.

phase shift of approximately -40°. In the low frequency limit $\Delta I/I = 2 \times 10^{-4}$. The concentration modulation of HO_2 in the low frequency limit is

$$\Delta[HO_2] = (P/Q)^{1/2}$$

$$= \left(\frac{4.5 \times 10^{12} \text{ molecules/cm}^3\text{.sec}}{7.1 \times 10^{-12} \text{cm}^3\text{/molecules.sec}}\right)^{1/2}$$

$$= 8 \times 10^{11} \text{ molecules/cm}^3$$

The optical path is 48 meters; the absorption coefficient to the base e is 5×10^{-20} cm^2/molecule. Because of uncertainties in the hydrogen peroxide concentration when the spectra was obtained, this figure may be in error by as much as a factor of two.

SECTION VIII

PHOTOLYSIS OF NITROGEN DIOXIDE

A. INTRODUCTION

The photolysis of nitrogen dioxide is a key reaction in photochemical air pollution[52], is important in stratospheric photochemistry,[53] and is often used in the laboratory to measure light intensity between 300 and 400 nm. The reaction is complex, and there is disagreement in the literature as to the value of certain rate constants and rate-constant ratios. There is agreement in the literature[54-56] that the following mechanism describes the overall kinetics of the photolysis of small amounts of NO_2 in an inert carrier gas.

	Reaction	Rate
a.	$NO_2 + h\nu \rightarrow NO + O(^3P)$	$\alpha I [NO_2]$
1.	$NO + O + M \rightarrow NO_2 + M$	$k_1 [M] [NO] [O]$
2.	$NO_2 + O \rightarrow NO + O_2$	$k_2 [NO_2] [O]$
3.	$NO_2 + O + M \rightarrow NO_3 + M$	$k_3 [M] [NO_2] [O]$
4.	$NO_3 + NO \rightarrow 2NO_2$	$k_4 [NO_3] [NO]$
5.	$NO_3 + NO_2 + M \rightarrow N_2O_5 + M$	$k_{5M} [NO_2] [NO_3]$
6.	$N_2O_5 + M \rightarrow NO_2 + NO_3 + M$	$k_{6M} [N_2O_5]$
7.	$O_2 + O + M \rightarrow O_3 + M$	$k_7 [M] [O_2] [O]$
8.	$NO + O_3 \rightarrow NO_2 + O_2$	$k_8 [NO] [O_3]$

The purpose of this study was to examine this system with the molecular technique, and in particular to focus on the rate constants for reactions 2, 3, and 4 at room temperature.

Quantities measured in this study were the decay of NO_2, the build-up and decay of N_2O_5, and the molecular modulation of NO_2 during intermittant illumination of a steady flow system. In terms of the mechanism these

measurements give the following information: At low pressures (below 50 torr) the M-gas dependent reactions (1 and 3) become negligible compared to reaction 2, and the decay of nitrogen dioxide can be described by

$$\left(\frac{d\ \ell n[NO_2]}{dt}\right)_{P\to O} = -2\ \alpha I \tag{23}$$

At one atmosphere total pressure and with small initial NO concentration, the disappearance of NO is given as a good approximation by

$$\ell n\ \frac{[NO_2]}{[NO_2]_o} = \frac{-2\alpha I t}{(1 + k_3[M]/k_2)} = -k_a t \tag{24}$$

where k_a is the empirical, first-order, decay constant. If the initial concentration of nitric oxide is close to zero, the initial rate of formation of dinitrogen pentoxide is

$$\left(\frac{d[N_2O_5]}{dt}\right)_{t\to 0} = \frac{\alpha I[NO_2]}{(1 + k_2/k_3[M])} \tag{25}$$

At an early stage of the reaction (t=t*) dinitrogen pentoxide goes through a maximum, at which point

$$\left(\frac{[N_2O_5]}{[NO_2]}\right)^* = \frac{\alpha I(K/k_4)}{(1 + k_2/k_3[M])}\ \ \frac{[NO_2]^*}{[NO]} \tag{26}$$

where $K = k_5/k_6$. The modulation amplitude of nitrogen dioxide in a steady flow system illuminated with square-wave photolyzing light of frequency f is

$$\left(\frac{\Delta[NO_2]}{[NO_2]}\right) = \frac{4\alpha I/\pi^2 f}{1 + \dfrac{k_1[NO]}{k_2[NO_2]} + \dfrac{k_3[M]}{k_2}} \tag{27}$$

It can be seen that Eq. 23 gives αI; with I so determined, Eqs. 24 and 25 give two independent measures of the ratio k_2/k_3; the combination of Eqs. 23, 24 and 27 gives k_1/k_2.

Thus by solving the five experimental relationships simultaneously, it is possible to obtain values for αI, k_4/K, k_1/k_2, and k_3/k_2, with one equation redundant to use as a check. By taking the literature values for k_1 and for the equilibrium constant K, it is possible to obtain the elementary rate constants $\underline{k}_2$, $\underline{k}_3$, $\underline{k}_4$.

B. RESULTS

A series of experiments was carried out in the closed cell with low total pressure, 19 to 56 torr; the decay of NO_2 was first-order throughout an experiment. When NO_2 is photolyzed in a closed cell at one atmosphere, the initial decay is first-order, but deviations from first-order kinetics appear at later times, as illustrated by Figure 32 (The concentration of NO_2 was followed by infrared absorption at 1600 cm^{-1}). The build up and decay of N_2O_5 is illustrated by Figure 33 for conditions at one atmosphere total pressure (N_2) and 24°C. The concentration of N_2O_5 was followed by infrared absorption at 1238 cm^{-1}. A plot of $([N_2O_5]/[NO_2])^*$ against $([NO_2]/[NO])^*$ is given as Figure 34, compare Eq. 26.

Along with these conventional measurements, a molecular-modulation study of NO_2 photolysis was carried out. The molecular-modulation method consists of monitoring the periodic concentration fluctuations induced in the reacting species by flashing the photolysis lamps on and off. In this work the NO_2 modulation was studied in a steady flow system with the photolysis lamps flashing at 1 cps. Under these conditions the NO_3 radicals and oxygen atoms will be at their steady state concentrations and N_2O_5 will be equilibrium.

The behavior of the concentration modulation of NO_2 can be described by a differential equation with the flashing lamps represented by the Fourier series for a square wave.

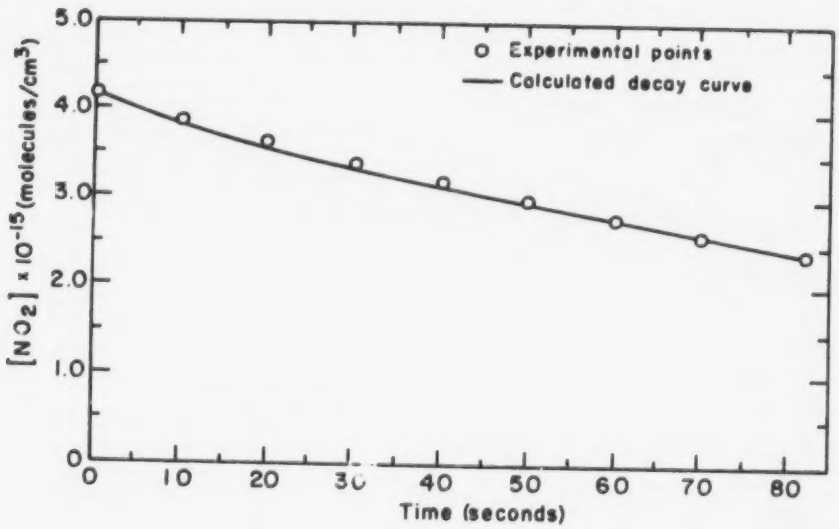

XBL728-6843

Figure 32 - NO_2 decay; comparison of experimental points and calculated curve based on rate constants in Table (5). Initial concentrations: $[NO_2] = 4.2 \times 10^{15}$, $[NO] = 2.05 \times 10^{14}$.

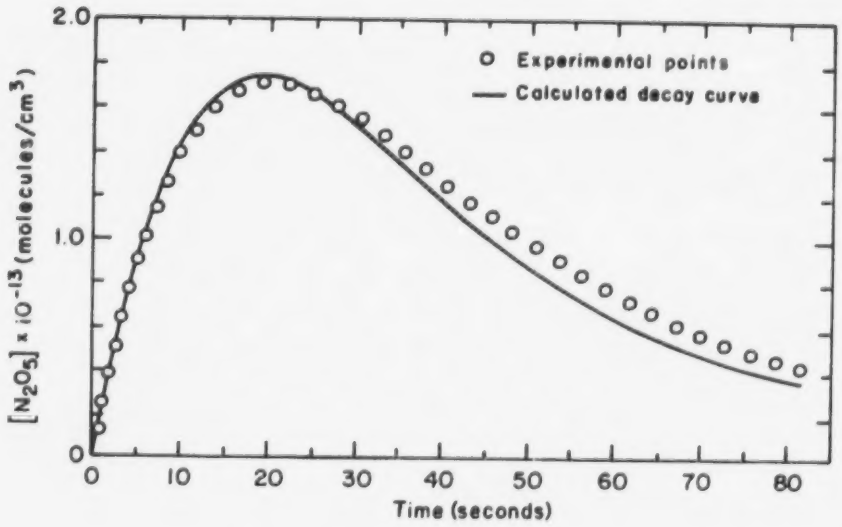

Figure 33 - N_2O_5 decay as observed by infrared absorption at 1237 cm^{-1}; comparison of experimental points and calculated curve based on rate constants in Table (5). Initial concentrations: NO_2 = 2.8×10^{15} molecules cm^{-3}, [NO] = 0.

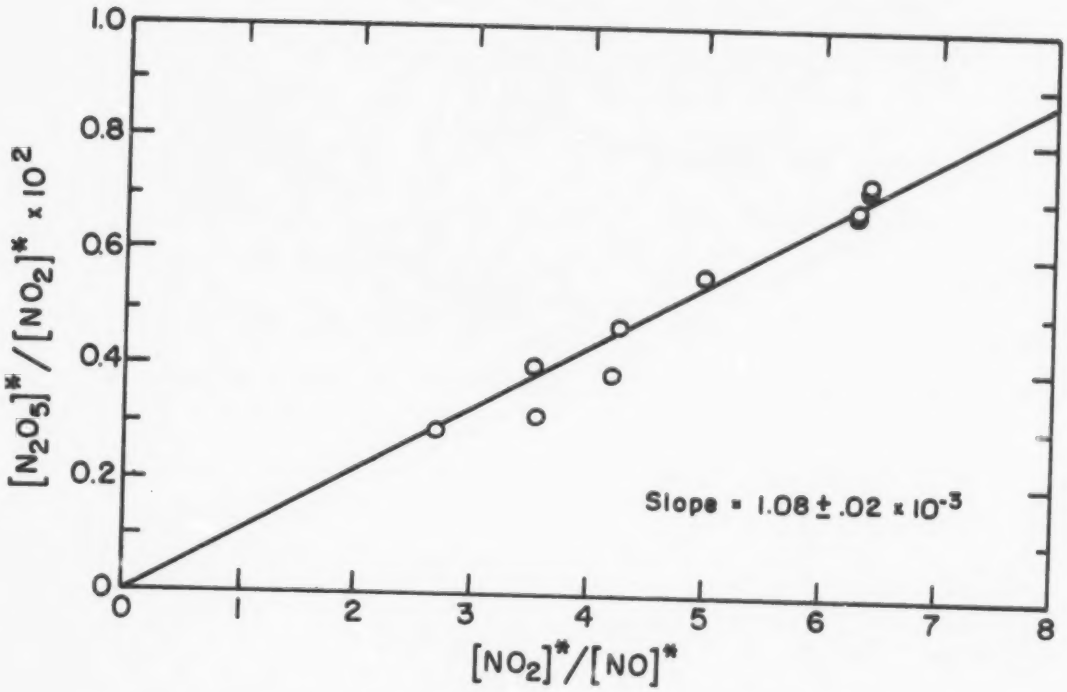

The * indicates the concentration at the time of the N_2O_5 concentration maximum, t^*

XBL 728-6842

Figure 34 - Concentration ratios where nitrogen pentoxide is a maximum, Equation 4.

$$\frac{d[NO_2]}{dt} = \frac{F}{V}\{[NO_2]_{in} - [NO_2]_{out}\} - \left(\frac{k_2[NO_2]^2}{k_1[NO]\ [M] + (k_2+k_3[M])\ [NO_2]}\right)$$

$$\left(\frac{2\alpha I}{\pi}\sum_{\text{odd } n}^{\infty}\frac{1}{n}\sin(n\omega t) + \alpha I\right) \qquad (28)$$

With: F = flow rate of chemicals

V = volume of the reaction cell

$[NO_2]_{in}$ = the NO_2 concentration flowing into the cell

$[NO_2]_{out}$ = the NO_2 concentration flowing out of the cell

$\omega = 2\pi/T$, where T is the period of the square wave

This equation neglects the ozone reactions, since the system contains no initial oxygen and the O_3 buildup will not be significant. Under these conditions the flow system has reached a steady state with respect to reactants and products, so the unmodulated or DC terms in Eq. 28 cancel leaving only the modulation or AC terms.

$$\frac{d[NO_2]_{AC}}{d\theta} = \frac{-\alpha I}{\pi^2 f}\ \frac{2k_2[NO_2]^2\sum_{\text{odd } n}^{\infty}\frac{1}{n}\sin(n\theta)}{k_1[NO]\ [M] + (k_2+k_3[M]\ [NO_2]} \qquad (29)$$

where $d\theta = 2\pi f dt$; $\theta = \omega t$; and f = flashing frequency.

Selecting the conditions so that the modulation will be less than one part per thousand leaves the reactant concentrations essentially constant, allowing Eq. 29 to be integrated in closed form to give:

$$[NO_2]_{AC} = \frac{\alpha I[NO_2]^2}{\pi^2 f}\ \frac{2k_2\sum_{\text{odd } n}^{\infty} n^{-2}\cos(n\theta)}{k_1[NO]\ [M] + (k_2+k_3[M]\ [NO_2]} \qquad (30)$$

By electronically filtering out all but the first Fourier component of the modulation signal, and taking the peak to peak amplitude gives the experimental relationship:

$$[NO_2]_{mod} = \frac{4\alpha I\ k_2[NO_2]^2}{\pi^2 f(k_1[NO][M]+k_2+k_3[M])[NO_2])} \qquad (31)$$

Comparison of Eqs. 30 and 28 shows the NO_2 modulation waveform to be triangular, phase shifted 90° from the exciting light. The amplitude of this waveform and its phase shift from the exciting light can be determined experimentally and related to Eq. 31.

A summary of the steady state concentrations with the phase shift and amplitude measurements are recorded in Table 5. The photolytic light intensity for the modulation experiments was found to be 11.2% greater than in the initial slope experiments, when measured by the phototransistor mounted in the cell, and the values of I have been normalized by this factor.

The observed rate constant ratios are assembled in Table 6. The two independent values of k_3/k_2 agree within 10 per cent; the value based on Eq. 24 was more precise and is preferred. This study gives only rate ratios, k_1/k_2, k_3/k_2, and k_4/K. To evaluate absolute values of rate constants, either k_1, k_2, or k_3 must be taken from the literature. Of the three, the most extensive and most precise data are those for k_1. From the literature, the value 6.9×10^{-32} cm^3 $molecule^{-1}$ sec^{-1} was taken for N_2 as foreign gas at room temperature. The observed quantity k_4/K is reduced to k_4 by the literature value of K. With these values of K and k_1, the elementary rate constants k_2, k_3, and k_4 are evaluated and listed in Table 7 with the other 8 elementary rate constants in this system.

With these 8 elementary reactions, a computer program was written that integrated the simultaneous rate equations to give NO_2 and N_2O_5 as a

Table 5. Data for NO_2 modulation at one atmosphere total pressure, 24°C.

Carrier gas	Steady state concentration $[NO_2]$ $\times 10^{-14}$	$[NO]$ $\times 10^{-15}$	k_a sec^{-1} $\times 10^{3}$	phase shift degrees	$\Delta[NO_2]$ mod. $\times 10^{-11}$	$\frac{k_1[M]}{k_2}$
N_2	1.02	0.74	8.3	93.6	1.43	0.163
N_2	1.19	1.22	8.3	89	1.31	0.179
N_2	0.68	1.49	8.3	70	1.40	0.189
N_2	1.13	2.04	8.3	82	0.83	0.185
N_2	1.87	2.12	8.3	80	1.62	0.190
N_2	1.68	1.60	7.2	94	1.68	0.178
Ar	1.55	1.38	8.3	88.2	1.78	0.190
Ar*	2.12	1.30	4.6	87.8	1.65	0.206
Ar	1.34	1.34	8.3	91.8	1.41	0.198

Table 6. Observed rate constant and rate constant ratios

Rate constant function	Observed value	Based on equation	Condition
αI	7.45×10^{-3} sec^{-1}	(1)	
k_a	1.22×10^{-2} sec^{-1}	(2)	1 atm N_2
$k_3[M]/k_2$	0.22	(2)	1 atm N_2
k_3/k_2	8.9×10^{21}	(2)	N_2 = M
$k_3[M]/k_2$	0.20	(3)	1 atm N_2
k_3/k_2	8.1×10^{21}	(3)	N_2 = M
k_4/K	0.71 sec^{-1}	(4)	
$k_1[M]/k_2$	0.18	(5)	1 atm N_2
k_1/k_2	7.3×10^{-21}	(5)	N_2 = M
$k_1[M]/k_2$	0.20	(5)	1 atm Ar
k_1/k_2	8.1×10^{-21}	(5)	Ar = M

Table 7. Elementary rate constants for nitrogen dioxide photolysis, 297°K, 1 atm N_2

Constant	Value	Source	Reference
k_1	6.9×10^{-32} cm^6 sec^{-1}	Literature	57-63
k_2	9.2×10^{-12} cm^3 sec^{-1}	k_1, k_1/k_2	Table 5
k_3	8.2×10^{-32} cm^6 sec^{-1}	k_2, k_3/k_2	Table 5
K	1.24×10^{-11} cm^{-3}	Literature	[64]
k_4	8.7×10^{-12} cm^3 sec^{-1}	k, k_4/K	Table 5
k_{6M}	0.104 sec^{-1}	Literature	[65]
k_{5M}	1.29×10^{-12} cm^3 sec^{-1}	K, k_{6M}	
k_7	6.24×10^{-34} cm^{-6} sec^{-1}	Literature	[66]
k_8	2.1×10^{-14} cm^3 sec^{-1}	Literature	[19]

function of time. In Figures 32 and 33 the circles represent observations and the smooth curves are those calculated from the elementary rate constants in Table 7. There is good agreement between the calculated and observed curves over the full course of observation.

SECTION IX

DISCUSSION

Solar radiation in the visible and near ultraviolet spectrum is "weak" relative to the radiation intensity from flash photolysis. The method of flash photolysis has been highly successful in obtaining the spectra and kinetics of free-radical intermediates in high intensity photochemical experiments. In a typical, complex photochemical reaction, there is competition between radical-molecule reactions (chain propagation) and radical-radical reactions (chain terminating, usually). The balance between these two competing processes is quite different under conditions of strong and weak light intensity. There is a distinct possibility that a given photochemical reaction will follow a different mechanism in the real sunlit world and in the laboratory using flash photolysis.

The molecular modulation method was designed to detect and follow free radicals in photochemical reactions at light intensities comparable to sunlight in intensity. With the first test of this method[1] new radicals were seen in the HO_x system (later shown to be the elusive HOO radical) and in the ClO_x system (still not positively identified but probably a complex of Cl, O_2, and CO). These radicals were detected at concentrations of about 10^{11} molecules cm^{-3} or less than one part per hundred million in the atmosphere. Design calculations based on light sources, light through-put in optical instruments, radical light-absorption cross sections, and detector sensitivity promised substantial improvements over this level of detection and routine analysis of reaction mechanisms at this level of radical concentration. Especially during the last phase of this grant, a new model of the molecular modulation apparatus was developed that (on paper) should have had greatly improved sensitivity, convenience, and flexibility. The light path was greatly extended, the monitoring infrared source was stabilized, the infrared detector was cold-shielded, and the electronics was set up in a digital mode, such that results could be recorded on paper tape or sent directly to a small computer.

The testing of this new improved system revealed a new, limiting source of error that overrides all of the improvements that were designed and made. The goal was to detect changes in the monitoring light beam at fractions of 10^{-6} to 10^{-5}. The infrared measuring beam has a long, folded, optical path of 100 meters or more. As the photolyzing lights are turned on and off, the light is absorbed by the primary reactant and heat is released to the carrier gas as free radical recombinations and reactions occur. These thermal effects, introducing time-varying and spatially non-uniform density gradients, appear to introduce noise to the long-path infrared beam. This noise restricts the usefulness of the molecular modulation method.

In the presence of this "accoustical noise", it is very time consuming and difficult to obtain molecular modulation data on free radical reactions at low intensities of photolyzing light. Even so, this report gives successful use of this method for the radicals HOO, ClOO, and ClO. The results for HOO have been confirmed by other studies[48,49], which used different experimental methods. The results for ClO and ClOO are quite different from those obtained by other methods (flash photolysis). There remains an unresolved conflict between these two methods. It may be that mechanism is quite different at low and at high light intensities, and there could be one or more unidentified elementary reaction responsible for the conflict. In view of the expected and observed difference in mechanisms at low and at high light intensities, it may be important to pursue the study of radical intermediates by the molecular-modulation method. However, it is so expensive in time and effort to make molecular-modulation studies that this method should be pursued only where there is a specific need for examing low-intensity photolysis. According to verbal reports, other groups (North American Research Center and Shell Research Laboratory of England) have adopted the molecular modulation method and used it with better success then that obtained here. In each case, they shortened the optical path to a meter or so and used photolysis lights 10 or 100 times more intense than sunlight. Such light intensities are still very small compared to flash photolysis. With a short optical path there is much less accoustical noise and there can be greater throughput of infrared radiation. With a chamber of small cross

section and small volume, there can be a much higher light intensity for photolysis.

In this laboratory, further work is being done on this method, but it is in the direction of shorter optical path and higher light intensity. The large apparatus built under this grant has been disassembled and rebuilt with the incorporation of these changes.

The goal of this project was to detect the CH_3OO and $CH_3(CO)OO$ radicals and to study their kinetics. This goal was not attained. This project did characterize spectra and kinetics of the HOO radical, and these data are useful for model calculations in the stratosphere and in the troposphere. This project characterized the ClOO and ClO radicals. This study was started simply as a calibration of the new method. Recently there has been a surprising development that makes ClO_x chemistry very much a matter of atmospheric chemistry. As is now well established, the oxides of nitrogen catalyze the destruction of stratospheric ozone by catalytic cycles including

$$NO + O_3 \rightarrow NO_2 \quad O_2$$
$$O_3 + h\nu \rightarrow O_2 + O$$
$$NO_2 + O \rightarrow NO + O_2$$
$$\text{net: } 2\,O_3 \longrightarrow 3\,O_2$$

In this cycle at typical stratospheric temperatures, NO_2 is 10,000 times as effective in destroying ozone as ozone itself. Recently it has been found that Cl and ClO undergo a similar cycle

$$Cl + O_3 \rightarrow ClO + O_2$$
$$O_3 + h\nu \rightarrow O_2 + O$$
$$ClO + O \rightarrow Cl + O_2$$
$$\text{net: } 2\,O_3 \longrightarrow 3\,O_2$$

The rate-determining step in this cycle has a rate constant 5 or 6 times larger than the rate determining step in NO_2 cycle. Thus one part of ClO is about 50,000 times as effective in destroying ozone as ozone itself. Recently it has been proposed that freons and other organic[68] chlorides released into the troposphere will eventually (decades) percolate into the upper stratosphere where they will be photolyzed to produce chlorine atoms. Thus the ClO_x chemistry studied here may have applications to atmospheric problems after all.

SECTION X

REFERENCES

1. Johnston, H. S., McGraw, G. E., Paukert, T. T., Richards, L. W. and Van den Bogaerde, J., Proc. Natl. Acad. Sci. U.S., 57 (1967) 1146.
2. Van den Bogaerde, J., Ph.D. Thesis, 1968, Univ. of Calif. Berkeley.
3. McGraw, G. E. and Johnston, H. S., J. Chem. Kinetics, 1 (1969) 89.
4. Paukert, T. T., Ph.D. Thesis, 1969, Univ. of Calif. Berkeley.
5. Morris, E. D., Jr., Ph.D. Thesis, 1969, Univ. of Calif. Berkeley.
6. Johnston, H. S., Morris, E. D., Jr. and Van den Bogaerde, J., J. Am. Chem. Soc., 91 (1969) 7712.
7. Morris, E. D., Jr. and Johnston, H. S., J. Am. Chem. Soc., 90 (1968) 1918.
8. Morris, E. D., Jr. and Johnston, H. S., Rev. Sci. Instr., 39 (1968) 620.
9. Wu, C. H., Ph.D. Thesis, 1969, Univ. of Calif., Berkeley.
10. Wu, C. H. and Johnston, H. S., Bull. Soc. Chem. Belges. 81 (1972), 135.
11. Bier, K. and Hagena, O., "In Rarefied Gas Dynamics," ed. J. A. Laurmann (1963), Academic Press, New York.
12. Margeneau, H., and Murphy, G. S., "The Mathematics of Physics and Chemistry", D. Van Nostrand Co., Inc., Princeton, N. J. (1956) p. 41.
13. Porter, G. and Wright, F. J., Disc. Faraday Soc., 14 (1953) 23.
14. Lipscomb, F. J., Norrish, R.G.W. and Thrush, B. A., Proc. Roy. Soc. A233, 455 (1956).
15. Edgecombe, F.H.C., Norrish, R.G.W., and Thrush, B. A., Proc. Roy. Soc. A243, 24 (1957).
16. McGrath, W. D., and Norrish, R.G.W., Proc. Roy. Soc. A254, 317 (1960).

17. Clyne, M.A.A., and Coxon, J. A., Trans. Faraday Soc. 62, 1175 (1966).

18. Durie, R. A. and Ramsay, D. A., Can. J. Phys. 36, 35 (1958).

19. Burns, G., and Norrish, R.G.W., Proc. Roy. Soc. A271, 289 (1963).

20. Benson, S. W., and Buss, J. H., J. Chem. Phys. 27, 1382 (1957).

21. Clyne, M.A.A., and Coxon, J. A., Proc. Roy. Soc. A303, 207 (1968).

22. Benson, S. W., Anderson, K. H., J. Chem. Phys. 31, 1082 (1959).

23. Rochkind, M. M., and Pimentel, G. C., J. Chem. Phys. 46, 4481 (1967).

24. Eachus, R. S., Edwards, P. R., Subramanian, S. and Symons, M.C.R., Chem. Communications 1967, 1036; J. Chem. Soc. (A) 1968, 1704.

25. Arkell, A., and Schwager, I., J. Am. Chem. Soc. 89, 5999 (1967).

26. Porter, G., Discussions Faraday Soc. 9, 60 (1950).

27. Marshall, A. L., J. Phys. Chem. 30, 34, 1078 (1926).

28. Taylor, H. S., Trans. Faraday Soc. 21, 560 (1926).

29. Lewis, B., and von Elbe, G., Third Symposium on Combustion and Flames and Explosion Phenomena, Williams and Wilkins Co., Baltimore, Md., (1949) p. 484.

30. Lewis, B., and von Elbe, G., "Combustion, Flames, and Explosions of Gases, Academic Press, New York (1961).

31. Baldwin, R. R., Mayor, L. and Doran, P., Trans. Faraday Soc. 56, 93 (1960).

32. Baldwin, R. R., and Mayor, L., Trans. Faraday Soc. 56, 80, 103 (1960).

33. Burgess, R. H., and Robb, J. C., Chem. Soc. Spec. Pub. No. 9, 167 (1957).

34. Heidt, L. J., and Forbes, G. S., J. Am. Soc. 56, 1671, 2365 (1934).

35. Volman, D. H., J. Am. Chem. Soc. 73, 1018 (1951).

36. Norrish, R.G.W., and Wayne, R. P., Proc. Roy. Soc. A288, 200 (1965).

37. McGrath, W. D., and Norrish, R.G.W., Proc. Roy. Soc. A254, 317 (1960).

38. Volman, D. H., Advances in Photochemistry 1, 43, Interscience Publ., New York (1963).

39. Volman, D. H., J. Chem. Phys. 17, 947 (1949).

40. Greiner, N. R., J. Chem. Phys. 45, 99 (1966); J. Phys. Chem. 72, 406 (1968).

41. Foner, S. N. and Hudson, R. L., J. Chem. Phys. 36, 2681 (1962); Foner, S. N., and Hudson, R. L., J. Chem. Phys. 21, 1608 (1953).

42. Robertson, A.J.B., Applied Mass Spectrometry, Institute of Petroleum, London (1954).

43. Ingold, K. U., and Bryce, W. A., J. Chem. Phys. 24, 360 (1956).

44. Fabian, D. J., and Bryce, W. A., Seventh International Symposium on Combustion, Butterworths Scientific Publications, London (1959) p. 150.

45. Milligan, D. E., and Jacox, M. E., J. Chem. Phys. 38, 2627 (1963) 40, 605 (1964).

46. Ogilvie, J. F., Spectrochimica Acta 23A, 737 (1967).

47. (a) Czapski, G. and Dorfman, L. M., J. Phys. Chem. 68, 1169 (1964); (b) Bielski, H. J. and Schwarz, H. A., J. Phys. Chem. 72, 3836 (1968); (c) Behar, D. and Czapski, G., Israel J. Chem. 8, 699 (1970).

48. Troe, J., Ber. Bunsengesellschaft Phys. Chem. 73, 946 (1969); also recent private communications.

49. Hochanadel, C. J., Ghormley, J. A., and Ogren, P. J., J. Chem. Phys. 56, 4426 (1972).

50. Holt, R. B., McLane, C. K., and Oldenberg, O. J. Chem. Phys. 16, 225, 638 (1948).

51. Urey, H. C., Dawsey, L. H., and Rice, F. O., J. Am. Chem. Soc. 51, 1371 (1929).

52. Hagen-Smit, A. J., Ind. Eng. Chem. 44, 1342 (1952).

53. (a) Nicolet, M., J. Geophys. Res. 70, 679 (1965). (b) Crutzen, P. J., Quart. J. Roy. Met. Soc. 96, 320 (1970). (c) Johnston, H. S., Science 173, 517 (1971).

54. Hall, T. C., Jr. "Photochemical Studies of Nitrogen Dioxide and Sulfur Dioxide", Doctoral Thesis, University of California, Los Angeles.

55. Ford, H. W. and Endow, N., J. Chem. Phys. 27, 1156, 1277 (1957).

56. Troe, J., Ber. Bunsenges. Physik Chem. 73, 906 (1969).

57. Kaufman, F., Proc. Roy. Soc. A247, 123 (1958).

58. Hartek, P. Reeves, R. R., and Mannella, G. G., Air Force Cambridge Research Center, Technical Report, AFCRC-TR60-264 (1960).

59. Clyne, M.A.A., and Thrush, B. A., Proc. Roy. Soc. A269, 404 (1962).

60. Ogryzlo, E. A., and Schiff, H. I., Can. J. Chem. 37, 1690 (1959).

61. Takahashi, S., and Miyazaki, S., Mem. Def. Acad., Jap. 8, 611 (1968).

62. Takahashi, S., Mem. Def. Acad., Jap. 8, 777 (1968).

63. Klein, F. S., and Herron, J. T., J. Chem. Phys. 41, 1285 (1964).

64. Schott, G., and Davidson, N., J. Am. Chem. Soc. 80, 1841 (1958).

65. Mills, R. L. and Johnston, H. S., J. Am. Chem. Soc. 73, 938 (1951).

66. Johnston, H. S., "Gas Phase Reaction Kinetics of Neutral Oxygen Species", NSRDS-National Bureau of Standards 20.

67. Johnston, H. S., and Crosby, H. J., J. Chem. Phys. 22, 689 (1954).

68. Molina, M. J., and Rowland, F. S., "Stratospheric Sink for Halogenated Hydrocarbons (Freons) - Chlorine Atom Catalyzed Destruction of Ozone", submitted to Nature, January 1974.